THE ASTRONOMICAL JOURNAL, 121:2189–2211, 2001 April

A CORONAGRAPHIC SURVEY FOR COMPANIONS OF STARS WITHIN 8 PARSECS

B. R. OPPENHEIMER[1]
Palomar Observatory, 105-24, California Institute of Technology, 1201 East California Boulevard, Pasadena, CA 91125
D. A. GOLIMOWSKI
Department of Physics and Astronomy, 3400 North Charles Street, Johns Hopkins University, Baltimore, MD 21218-2686
S. R. KULKARNI, K. MATTHEWS, T. NAKAJIMA,[2] AND M. CREECH-EAKMAN
Palomar Observatory, 105-24, California Institute of Technology, 1201 East California Boulevard, Pasadena, CA 91125
AND
S. T. DURRANCE[3]
Department of Physics and Astronomy, 3400 North Charles Street, Johns Hopkins University, Baltimore, MD 21218-2686
Received 2000 June 20; accepted 2000 December 27

ABSTRACT

We present the technique and results of a survey of stars within 8 pc of the Sun with declinations $\delta > -35°$ (J2000.00). The survey, designed to find without color bias faint companions, consists of optical coronagraphic images of the 1′ field of view centered on each star and infrared direct images with a 32″ field of view. The images were obtained through the optical Gunn r and z filters and the infrared J and K filters. The survey achieves sensitivities up to 4 absolute magnitudes fainter than the prototype brown dwarf, Gliese 229B. However, this sensitivity varies with the seeing conditions, the intrinsic brightness of the star observed, and the angular distance from the star. As a result, we tabulate sensitivity limits for each star in the survey. We used the criterion of common proper motion to distinguish companions and to determine their luminosities. In addition to the brown dwarf Gl 229B, we have identified six new stellar companions of the sample stars. Since the survey began, accurate trigonometric parallax measurements for most of the stars have become available. As a result, some of the stars we originally included should no longer be included in the 8 pc sample. In addition, the 8 pc sample is incomplete at the faint end of the main sequence, complicating our calculation of the binary fraction of brown dwarfs. We assess the sensitivity of the survey to stellar companions and to brown dwarf companions of different masses and ages.

Key words: binaries: visual — stars: low-mass, brown dwarfs — stars: statistics

1. INTRODUCTION

In 1992, a brown dwarf companion search began at Palomar with the initiation of a collaboration between T. N. and S. R. K. at Caltech and D. A. G. and S. T. D. at Johns Hopkins. The Hopkins group brought the Adaptive Optics Coronagraph (AOC; Golimowski et al. 1992) to Palomar to be fitted on the 60 inch (1.5 m) telescope. The first results of this collaboration were given in Nakajima et al. (1994), which entailed a search for companions of high Galactic latitude stars. Companions were distinguished from background stars through statistical arguments based on the distribution of point sources as a function of angular separation from the stars. In 1994, the work expanded to a new sample of nearby stars that were believed to be young. A short description of this sample is contained in Nakajima et al. (1995). This sample was biased toward young stars in an attempt to discover brown dwarf companions, with the assumption that younger brown dwarfs would be easier to detect because they should be brighter (Oppenheimer, Kulkarni, & Stauffer 2000). The first success of this collaboration was the discovery of a faint companion of the star Gliese 105A (Golimowski et al. 1995). The first success of the young-star survey was the discovery of the cool brown dwarf Gliese 229B (Nakajima et al. 1995; Oppenheimer et al. 1995).

Following the discovery of Gl 229B, we decided that it was of paramount importance to conduct a volume-limited survey for companions. If we continued to pursue the biased sample and found no more brown dwarfs, we would have little to say about the prevalence of companion brown dwarfs without extensive modeling.

For this reason, in late 1994 we began a survey of all the northern ($\delta > -35°$) stars within 8 pc of the Sun to search for brown dwarf companions. Because all of the known stars within 8 pc have measurable proper motions, our survey was designed to find common proper motion companions. We thus observed each star at multiple epochs, if point sources other than the star appeared in the field of view. This permitted us to discern companions simply by measuring the relative offset between the star and the putative companions at each epoch. The common proper motion criterion, almost 50 years old now, is ideal in searches for brown dwarfs because it is intrinsically unbiased by color or other theoretical notions of what a brown dwarf should look like. (Other systematic searches for companions that used the common proper motion criterion are by Van Biesbroeck 1961, Luyten 1977, Skrutskie, Forrest, & Shure 1989, Simons, Henry, & Kirkpatrick 1996, Koerner et al. 1999, and Schroeder et al. 2000; see Oppenheimer et al.

[1] Current address: Department of Astronomy, 601 Campbell Hall, University of California at Berkeley, Berkeley, CA 94720-3411; bro@astron.berkeley.edu.
[2] Current address: National Astronomical Observatory, Tenmondai, 2-21-1 Osawa, Mitaka, Tokyo 181, Japan.
[3] Current address: Florida Space Institute, Mail Stop FSI, Kennedy Space Center, FL 32899.

2000 for a description of the history of brown dwarf searches.) The common proper motion criterion is the most physically rigorous short-term method for finding companions. (Longer term methods include orbital motion measurements and common parallax measurements, which eliminate the minute possibility that two objects within an arcminute of each other might exhibit common proper motion and yet be physically unassociated.)

This survey is also distinguished from others because it represents the first use of adaptive optics techniques in the study of nearby stars. With our tip-tilt observations dating back to 1992, we greatly predate any other such searches. At the time of this writing, the use of higher order adaptive optics systems is becoming widespread in these sorts of studies (e.g., Delfosse et al. 1999). The combination of adaptive optics and coronagraphy, and the use of both infrared and optical bandpasses, made our search effective. We demonstrate in § 9 and Figure 19 that the survey covers previously unobserved parts of the companion mass-separation parameter space.

To achieve our goal of a volume-limited survey, we assembled a sample of stars that appear in the Third Catalogue of Nearby Stars (Gliese & Jahreiss 1991) and have parallaxes greater than 0″.125. The degree of completeness of this sample has been the subject of debate (see, e.g., Reid & Gizis 1997). We address this issue in depth in § 2, where we also present an updated catalog of the stars within 8 pc. The observations are explained in detail in § 3, and a complete description of the sensitivity limits is presented in following sections.

2. THE 8 PARSEC SAMPLE

2.1. *Culling the Catalog*

When we began our survey, the best list of stars within 8 pc of the Sun was a subset of the Third Catalogue of Nearby Stars (CNS3; Gliese & Jahreiss 1991). The subsequent releases of the *Hipparcos* main catalog (Perryman et al. 1997) and the Yale catalog of trigonometric parallaxes (van Altena, Lee, & Hoffleit 1995) provide important sets of data that modify the census of stars within 8 pc. Ultimately the two new catalogs moved some stars out of, and others into, the 8 pc sample. These catalogs also added a few stars to the sample, which were not in the CNS3. The *Hipparcos* Catalogue did not add any unknown stars to the 8 pc sample, because trigonometric parallaxes were only obtained for previously cataloged stars. However, *Hipparcos* did measure seven stars in five systems whose parallaxes had never before been measured and which place them within 8 pc. The Yale catalog adds no new stars to the sample but does provide trigonometric parallaxes for 37 stars within 8 pc that were not measured by *Hipparcos*. This reduces the number of stars in our sample whose parallaxes are simply inferred from photometry. These so-called photometric parallaxes involve measurements of the colors of a given star. The colors determine the spectral class of the star and, thus, its absolute luminosity. From the absolute luminosity, the distance modulus is calculated. These photometric parallaxes are sometimes inaccurate because of unknown multiplicity and intrinsic scatter in the main sequence, which can lead to errors in the distance as large as 30% (Weis 1984). In the new catalog we assemble here, only six stars are included based on photometric parallaxes. These are the only stars within 8 pc in the CNS3 that were not measured astrometrically by the *Hipparcos* or the Yale survey.

Pursuant to this discussion, we have created a new catalog of stars within 8 pc of the Sun. We believe this constitutes the most complete census of the northern 8 pc volume to date. In our catalog, we combine all the stars within the CNS3 and *Hipparcos* and Yale catalogs that have parallaxes greater than 0″.125. The three catalogs are fully cross-correlated, and for each entry in our database we have up to three different parallaxes, although only the most accurate is listed in the catalog presented here. Precedence for inclusion in the final catalog is given to the *Hipparcos* measurement, which is generally more accurate than the Yale measurement (except in the case of star systems Gl 185AB and Gl 644ABCD, where the Yale parallax is more accurate). For six of the stars, neither Yale nor *Hipparcos* measurements exist. These stars have photometric parallaxes listed in the CNS3, and we list them to be as inclusive as possible.

To be certain that we have included all the known subordinate stellar and substellar objects associated with these stars, we conducted a search of the literature. Two papers in particular (Delfosse et al. 1999; Reid & Gizis 1997) provided new companions, some of which have been resolved and some of which were detected through radial velocity studies. Our catalog is not biased in any way as to whether a given companion has been visually resolved. A complete census must be free of these considerations. Therefore, we include all of the companions mentioned in Reid & Gizis (1997) and most of those in Delfosse et al. (1999). We believe that our final catalog is complete as of 2000 January because we have used all the available resources and studies of the nearby stars.

Our sample includes, therefore, 163 stars, two brown dwarfs (Nakajima et al. 1995; Burgasser et al. 2000), and one indirectly detected planet (Delfosse et al. 1998). These entities are arranged in 111 star systems, 29 of which are double, nine of which are triple, two of which are quadruple, and one of which is quintuple.

Table 1 lists all the star systems in the 8 pc sample described above. In this table, we give a single entry for every object known within 8 pc. For multiple systems, entries are grouped together and indicate the separation of the subordinate components, along with other vital data. The table is arranged in order of decreasing parallax in milliarcseconds. The "Source Code" field in each entry indicates where the parallax measurement comes from. Companions of stars are indicated by capital roman letters after the parallax and generally are given in the order in which the components were discovered. An implicit "A" is given to the principal star in each star system. However, the A is only used if at least component B has been discovered. For convenience we give HD, Durchmusterung, CNS3, or other names for the stars if they are available. This permits easy identification of the stars in astronomical databases.

2.2. *Completeness of the* 8 pc *Catalog*

It is important, before describing the observations we undertook, to estimate how complete our catalog of star systems within 8 pc is.

The simplest way to assess this involves extrapolating the number of stars within 5 pc to the volume of the 8 pc sample. This sort of analysis was conducted by Henry et al. (1997). In their estimation, the CNS3 is complete for stars

TABLE 1

THE 8 pc SAMPLE

PARALLAX (mas)	POSITION (J2000.00) R.A.	Decl.	μ (mas) R.A.	Decl.	V (mag)	CNS3 NAME	DURCHMUSTERUNG	OTHER NAME	SMA (AU)	SOURCE CODE
549.01.....	17 57 48.50	+04 41 36.2	−797.84	10326.93	9.54	Gl 699	BD +04°3561	G140-024	...	HHH
419.10.....	10 56 22.46	+07 00 27.6	−3846.7	−2693.5	13.46	Gl 406	...	G045-020	...	YYY
392.40.....	11 03 20.19	+35 58 11.6	−580.20	−4767.09	7.49	Gl 411	BD +36°2147	G119-052	...	HHH
379.21A.....	06 45 08.92	−16 42 58.0	−546.01	−1223.08	−1.44	Gl 244A	BD −16 1591	...	...	HHH
379.21B.....	...	...	...	...	8.44	Gl 244B	...	...	19.7	HHC
373.70A.....	01 39 01.74	−17 56 58.5	3316.8	584.8	12.52	Gl 65A	...	G272-061	...	YYY
373.70B.....	...	...	...	...	12.56	Gl 65B	...	...	5.1	YYY
336.48.....	18 49 49.36	−23 50 10.4	637.55	−192.47	10.37	Gl 729	...	...	...	HHH
316.00.....	23 41 56.69	+44 09 34.5	84.6	−1614.8	12.27	Gl 905	...	G171-010	...	YYY
310.75.....	03 32 55.84	−09 27 29.7	−976.44	17.97	3.72	Gl 144	BD −09°697	...	...	HHH
299.58.....	11 47 44.40	+00 48 16.4	605.62	−1219.23	11.12	Gl 447	...	G010-050	...	HHH
289.50A.....	22 38 37.25	−15 17 07.1	2379.8	2219.2	12.32	Gl 866A	...	G156-031	...	YYY
289.50B.....	...	...	...	...	...	Gl 866B	...	G156-031B	1.2	YY
289.50C.....	...	...	...	...	...	Gl 866C	...	G156-031C	0.3	YY
287.13A.....	21 06 53.94	+38 44 57.9	4155.10	3258.90	5.20	Gl 820A	BD +38°4343	...	...	HHH
285.42B.....	21 06 55.26	+38 44 31.4	4107.40	3143.72	6.05	Gl 820B	BD +38°4344	...	85.2	HHH
285.93A.....	07 39 18.12	+05 13 30.0	−716.57	−1034.58	0.40	Gl 280A	BD +05°1739	...	...	HHH
285.93B.....	...	...	...	...	10.7	Gl 280B	...	...	15.9	HHC
280.28A.....	18 42 46.69	+59 37 49.4	−1326.88	1802.12	8.94	Gl 725A	BD +59°1915	G227-046	...	HHH
284.48B.....	18 42 46.90	+59 37 36.6	−1393.20	1845.73	9.70	Gl 725B	...	G227-047	48.5	HHH
280.27A.....	00 18 22.89	+44 01 22.6	2888.92	410.58	8.09	Gl 15A	BD +43°44	G171-047	...	HHH
280.27B.....	...	...	...	...	11.06	Gl 15B	...	G171-048	155.0	HHC
275.80.....	08 29 44.30	+26 46 01.4	−1139.0	−605.6	14.81	GJ 1111	...	G051-015	...	YYY
274.17.....	01 44 04.08	−15 56 14.9	−1721.82	854.07	3.49	Gl 71	BD −16°295	...	...	HHH
269.05.....	01 12 30.64	−16 59 56.3	1210.09	646.95	12.10	Gl 54.1	...	G268-135	...	HHH
263.26.....	07 27 24.50	+05 13 32.8	571.27	−3694.25	9.84	Gl 273	BD +05°1668	G089-019	...	HHH
249.52A.....	22 27 59.47	+57 41 45.1	−870.23	−471.10	9.59	Gl 860A	BD +56°2783	G232-075	...	HHH
249.52B.....	...	...	...	...	9.85	Gl 860B	...	...	9.5	HHY
242.89A.....	06 29 23.40	−02 48 50.3	694.73	−618.62	11.12	Gl 234A	...	G106-049	...	HHH
242.89B.....	...	...	...	...	14.6	Gl 234B	...	...	4.2	HHC
235.24A.....	14 49 32.61	−26 06 20.5	−1389.70	135.76	11.72	Gl 563.2A	CD −25°10553	...	...	HHH
221.80B.....	14 49 31.76	−26 06 42.0	−1421.60	−203.60	12.07	Gl 563.2B	...	...	5.4	HHH
234.51.....	16 30 18.06	−12 39 45.3	−93.61	−1184.90	10.10	Gl 628	BD −12°4523	G153-058	...	HHH
227.90A.....	12 33 16.37	+09 01 16.1	−1797.5	220.7	12.44	Gl 473A	...	G012-043	...	YYY
227.90B.....	...	...	...	...	13.04	Gl 473B	...	...	5.4	YYY
227.45.....	03 22 05.50	−13 16 43.8	−112.94	−299.04	12.16	...	...	HIP 15689	...	HHH
226.95.....	00 49 09.90	+05 23 19.0	1233.05	−2710.56	12.37	Gl 35	...	G001-027	...	HHH
224.80.....	02 00 05.90	+13 00 34.2	1111.2	−1778.4	12.26	Gl 83.1	...	G003-033	...	YYY
224.00A.....	08 58 56.10	+08 28 28.0	329.1	−320.0	10.89	1405A	...	G041-014A	...	GCC
224.00B.....	...	...	...	...	...	1405B	...	G041-014B	0.5	GC
224.00C.....	...	...	...	...	...	1405C	...	G041-014C	3.2	GC
220.85.....	17 36 25.90	+68 20 20.9	−320.47	−1269.55	9.15	Gl 687	BD +68°946	G240-063	...	HHH
220.30.....	10 48 15.29	−11 21 30.5	616.2	−1525.2	15.60	1679	...	...	...	YYY
220.20A.....	19 53 56.51	+44 24 14.6	439.9	−583.8	13.41	GJ 1245A	...	G208-044	...	YYY
220.20B.....	...	...	...	...	14.01	GJ 1245B	...	G208-045	47.0	YYC
220.20C.....	...	...	...	...	13.41	GJ 1245C	...	G208-044B	3.7	YYC
213.00.....	00 06 39.52	−07 34 18.5	−830.1	−1864.5	13.74	GJ 1002	...	G158-027	...	YYY
212.69A.....	22 53 16.73	−14 15 49.3	960.33	−675.64	10.16	Gl 876A	BD −15°6290	G156-057A	...	HHH
212.69B.....	22 53 16.73	−14 15 49.3	960.33	−675.64	...	Gl 876B	BD −15°6290	G156-057B	0.21	HH
206.94A.....	11 05 28.58	+43 31 36.4	−4410.79	943.32	8.82	Gl 412A	BD +44°2051	G176-011	...	HHH
206.94B.....	...	...	...	...	14.40	Gl 412B	...	G176-012	190.0	HHC
205.22.....	10 11 22.14	+49 27 15.3	−1361.55	−505.00	6.60	Gl 380	BD +50°1725	G196-009	...	HHH
204.60.....	10 19 36.23	+19 52 10.7	−503.2	−52.9	9.40	Gl 388	BD +20°2465	G054-023	...	YYY
202.69.....	17 29 36.25	+24 39 14.7	97.33	348.92	11.39	...	...	HIP 85605	...	HHH
198.24A.....	04 15 16.32	−07 39 10.3	−2239.33	−3419.86	4.43	Gl 166A	BD −07°780	...	...	HHH
198.24B.....	...	...	...	...	9.52	Gl 166B	BD −07°781	G160-060	507.5	HHC
198.24C.....	...	...	...	...	11.17	Gl 166C	...	...	44.5	HHC
198.00A.....	22 46 48.50	+44 19 50.6	−772.3	−464.0	10.06	Gl 873A	BD +43°4306	...	...	YYY
198.07B.....	22 46 49.73	+44 20 02.4	−704.66	−459.39	10.29	Gl 873B	BD +43°4305	G216-016	167.4	HHH
196.62A.....	18 05 27.29	+02 30 00.4	124.56	−962.66	4.03	Gl 702A	BD +02°3482	...	...	HHH
196.62B.....	...	...	...	...	4.20	Gl 702B	...	...	22.9	HHY
194.44.....	19 50 47.00	+08 52 06.0	536.82	385.54	0.76	Gl 768	BD +08°4236	...	...	HHH

TABLE 1—*Continued*

Parallax (mas)	Position (J2000.00)		μ (mas)		V (mag)	CNS3 Name	Durchmusterung	Other Name	SMA (AU)	Source Code
	R.A.	Decl.	R.A.	Decl.						
191.86A	00 15 28.11	−16 08 01.7	728.18	−617.48	11.49	GJ 1005A	...	G158-050A	...	HHH
191.86B	...	...	...	...	...	GJ 1005B	...	G158-050B	3.9	HH
191.20A	08 58 12.21	+19 45 45.9	−873.5	−30.5	14.06	GJ 1116A	...	G009-038	...	YYY
191.20B	...	...	...	...	14.92	GJ 1116B	...	...	23.6	YYC
186.20	06 00 03.23	+02 42 15.6	229.2	−74.5	11.33	0999	...	G099-049	...	YYY
185.48	11 47 41.38	+78 41 28.2	743.21	480.40	10.80	Gl 445	...	G254-029	...	HHH
184.13	13 45 43.78	+14 53 29.5	1778.46	−1455.52	8.46	Gl 526	BD +15°2620	G063-053	...	HHH
182.15	20 52 33.02	−16 58 29.1	−306.70	30.78	11.41	...	...	HIP 103039	...	HHH
181.36A	04 31 11.52	+58 58 37.5	1300.21	−2048.99	10.82	Gl 169.1A	...	G175-034	...	HHH
181.36B	...	...	...	...	12.44	Gl 169.1B	...	G175-034	46.6	HHC
181.32	06 54 48.96	+33 16 05.4	−729.33	−399.31	9.89	Gl 251	...	G087-012	...	HHH
177.46	10 50 52.06	+06 48 29.3	−804.40	−809.60	11.64	Gl 402	...	G044-040	...	HHH
175.72	05 31 27.40	−03 40 38.0	763.05	−2092.89	7.97	Gl 205	BD −03°1123	G099-015	...	HHH
173.41	19 32 21.59	+69 39 40.2	598.43	−1738.81	4.67	Gl 764	BD +69°1053	...	...	HHH
173.19A	06 10 34.62	−21 51 52.7	−137.01	−714.06	8.15	Gl 229A	BD −21°1377	...	...	HHH
173.19B	...	...	...	...	...	Gl 229B	...	...	48.8	HH
172.78	05 42 09.27	+12 29 21.6	1999.05	−1570.64	11.56	Gl 213	...	G102-022	...	HHH
170.26A	19 16 55.26	+05 10 08.1	−578.86	−1331.70	9.12	Gl 752A	BD +04°4048	G022-022	...	HHH
170.26B	...	...	...	...	17.52	Gl 752B	...	...	521.6	HHC
169.90	08 12 41.57	−21 33 11.6	37.0	−706.0	12.10	Gl 300	...	...	...	YYY
169.32A	14 57 28.00	−21 24 55.7	1034.18	−1725.60	5.72	Gl 570A	BD −20°4125	...	...	HHH
163.63B	14 57 26.54	−21 24 41.5	987.05	−1666.81	8.01	Gl 570B	BD −20°4123	...	107.5	HHH
163.63C	14 57 26.54	−21 24 41.5	987.05	−1666.81	...	Gl 570C	...	...	0.8	HH
169.32D	14 57 28.34	−21 26 13.5	987.05	−1666.81	...	Gl 570D	...	...	1400	HH
168.59	07 44 40.17	+03 33 08.8	−344.87	−450.84	11.19	Gl 285	...	G050-004	...	HHH
167.99A	00 49 06.29	+57 48 54.7	1087.11	−559.65	3.46	Gl 34A	BD +57°150	...	...	HHH
167.99B	...	...	...	...	7.51	Gl 34B	...	...	71.00	HHC
167.51	23 49 12.53	+02 24 04.4	995.12	−968.25	8.98	Gl 908	BD +01°4774	G029-068	...	HHH
167.08A	17 15 20.98	−26 36 10.2	−473.69	−1143.93	4.33	Gl 663A	CD −26°12026	...	...	HHH
167.08B	17 15 20.98	−26 36 10.2	−473.69	−1143.93	5.11	Gl 663B	...	...	74.0	HHC
167.56C	17 16 13.36	−26 32 46.1	−479.71	−1123.37	6.33	Gl 664	CD −26°12036	...	6390.0	HHH
164.70	17 47 51.02	+70 53 46.3	−1246.0	1083.2	14.15	GJ 1221	...	G240-072	...	YYY
163.51	14 34 16.81	−12 31 10.4	−357.50	595.12	11.32	Gl 555	BD −11°3759	...	...	HHH
163.00	05 01 57.60	−06 56 42.0	−541.8	−551.3	12.1	0855	...	...	...	GCC
162.50	12 13 25.87	+10 15 43.5	−92.8	−14.7	5.85	1922	BD +11°2440	...	...	YYY
162.00A	07 36 25.00	+07 04 44.0	203.0	−290.0	13.22	1201A	...	G089-032A	...	GCC
162.00B	...	...	...	...	13.22	1201B	...	G089-032B	3.5	GCC
161.77A	17 46 14.41	−32 06 08.3	−77.62	−270.12	11.39	...	...	HIP 86963A	...	HHH
161.77B	17 46 12.63	−32 06 12.8	−49.82	−319.82	10.49	...	...	HIP 86963B	155.0	HHH
161.77C	17 46 14.41	−32 06 08.3	−77.62	−270.12	...	...	...	HIP 86963C	<0.1	HH
161.59A	09 14 22.79	+52 41 11.8	−1533.58	−562.80	7.64	Gl 338A	BD +53°1320	G195-017	...	HHH
159.48B	09 14 24.70	+52 41 11.0	−1551.30	−656.25	7.70	Gl 338B	BD +53°1321	G195-018	102.0	HHH
160.06A	23 31 52.18	+19 56 14.1	554.40	−62.61	10.05	Gl 896A	BD +19°5116	G068-024	...	HHH
160.06B	...	...	...	...	12.4	Gl 896B	...	...	25.8	HHC
160.06C	...	...	...	...	...	Gl 896C	...	...	<0.1	HH
160.06D	...	...	...	...	...	Gl 896D	...	...	<0.1	HH
159.52	15 19 26.82	−07 43 20.2	−1224.55	−99.52	10.57	Gl 581	BD −07°4003	G151-046	...	HHH
158.17A	17 12 07.89	+45 39 57.5	325.96	−1591.73	9.31	Gl 661A	BD +45°2505	G203-051	...	HHH
158.17B	...	...	...	...	9.96	Gl 661B	...	...	4.4	HHY
157.24A	07 10 01.83	+38 31 46.1	−439.68	−948.36	11.65	Gl 268A	...	G087-026	...	HHH
157.24B	...	...	...	...	...	Gl 268B	...	...	0.1	HH
156.30	14 56 38.58	−30 10 33.6	−482.5	−835.7	17.05	2363	...	...	...	YYY
156.00	13 07 04.30	+20 48 38.0	−71.7	−39.8	12.58	GJ 2097	...	...	...	GCC
155.00	05 55 09.37	−04 10 04.6	534.7	−2316.1	14.45	Gl 223.2	...	G099-044	...	YYY
153.96A	16 55 28.75	−08 20 10.8	−829.34	−878.81	9.02	Gl 644A	BD −08°4352	...	...	YHH
153.96B	16 55 28.75	−08 20 10.8	−829.34	−878.81	9.69	Gl 644B	...	...	1.4	YHY
153.96C	16 55 31.75	−08 23 38.8	−829.34	−878.81	16.78	Gl 644C	...	...	1765.0	YHC
153.96D	16 55 28.75	−08 20 10.8	−829.34	−878.81	...	Gl 644D	...	...	0.1	YHH
153.96E	16 55 25.23	−08 19 21.3	−813.47	−895.23	11.73	Gl 643	...	...	557.8	HHH
153.24	23 13 16.98	+57 10 06.1	2074.37	294.97	5.57	Gl 892	BD +56°2966	...	...	HHH
152.90	12 18 54.77	+11 07 41.4	−1285.0	203.5	13.79	GJ 1156	...	G012-030	...	YYY
151.93	16 25 24.62	+54 18 14.8	432.29	−170.71	10.13	Gl 625	...	G202-048	...	HHH
150.96	11 00 04.26	+22 49 58.7	−426.31	−279.94	10.03	Gl 408	...	G058-032	...	HHH
149.26A	14 51 23.38	+19 06 01.7	152.81	−71.28	4.54	Gl 566A	BD +19°2870	...	...	HHH

TABLE 1—*Continued*

Parallax (mas)	Position (J2000.00) R.A.	Position (J2000.00) Decl.	μ (mas) R.A.	μ (mas) Decl.	V (mag)	CNS3 Name	Durchmusterung	Other Name	SMA (AU)	Source Code
149.26B.....	...	...	...	...	6.97	Gl 566B	...	...	32.7	HHC
148.29A.....	21 29 36.81	+17 38 35.8	1008.09	376.21	10.33	Gl 829A	...	G126-004A	...	HHH
148.29B.....	...	...	...	...	...	Gl 829B	...	G126-004B	0.5	HH
146.30.....	08 12 03.21	+08 44 41.3	1172.2	−5077.4	12.83	Gl 299	...	G050-022	...	YYY
145.27.....	22 56 34.81	+16 33 12.4	−1033.21	−283.33	8.68	Gl 880	BD +15°4733	G067-037	...	HHH
143.45A.....	17 18 57.18	−34 59 23.3	1149.24	−90.80	5.91	Gl 667A	CD −34°11626	...	...	HHH
143.45B.....	...	...	...	...	6.27	Gl 667B	...	...	5.0	HHY
143.45C.....	...	...	...	...	10.24	Gl 667C	...	...	34.0	HHC
141.95.....	20 53 19.79	+62 09 15.8	1.08	−774.24	8.55	Gl 809	BD +61°2068	G231-019	...	HHH
138.72A.....	02 36 04.89	+06 53 12.7	1806.27	1442.50	5.79	Gl 105A	BD +06°398	G073-070A	...	HHH
138.72B.....	02 36 14.20	+06 52 06.0	1806.27	1442.50	5.82	Gl 105B	...	G073-071	1588.0	HGY
138.72C.....	02 36 04.89	+06 53 12.7	1806.27	1442.50	...	Gl 105C	BD +06°398B	G073-070B	28.8	HH
138.30.....	23 35 14.37	−02 24 12.6	789.1	−846.2	14.69	GJ 1286	...	G157-077	...	YYY
138.29.....	10 28 55.55	+00 50 27.6	−602.32	−731.87	9.65	Gl 393	BD +01°2447	G055-024	...	HHH
137.84A.....	17 09 31.54	+43 40 52.9	333.92	−278.02	11.77	2708A	...	G203-047A	...	HHH
137.84B.....	...	...	...	...	...	2708B	...	G203-047B	3.0	HH
137.50.....	18 19 02.56	+66 11 06.1	470.2	−408.7	13.46	2897	...	G258-033	...	YYY
135.30A.....	00 24 41.30	−27 08 52.8	−53.5	611.7	15.42	GJ 2005A	...	...	...	YYY
135.30B.....	...	...	...	...	...	GJ 2005B	...	...	7.39	YY
135.30C.....	...	...	...	...	...	GJ 2005C	...	...	14.80	YY
134.40.....	22 23 07.54	−17 37 01.1	291.4	−721.3	13.25	3517	...	...	...	YYY
134.04.....	00 48 22.98	+05 16 50.2	758.04	−1141.22	5.74	Gl 33	BD +04°123	...	...	HHH
133.91.....	01 42 29.76	+20 16 06.6	−302.12	−677.40	5.24	Gl 68	BD +19°279	...	...	HHH
132.60.....	18 07 30.80	−15 58 14.2	−563.1	−351.9	13.64	GJ 1224	...	G154-044	...	YYY
132.42.....	02 44 15.51	+25 31 24.1	864.77	−367.17	10.55	Gl 109	...	G036-031	...	HHH
132.40A.....	01 08 16.39	+54 55 13.2	3421.44	−1599.27	5.17	Gl 53A	BD +54°223	...	...	HHH
132.40B.....	...	...	...	...	11	Gl 53B	...	...	4.8	HHC
132.10.....	06 01 11.30	+59 35 00.2	−144.3	−818.4	11.71	0998	...	G192-013	...	YYY
131.12.....	13 29 59.79	+10 22 37.8	1128.00	−1074.30	9.05	Gl 514	BD +11°2576	G063-034	...	HHH
130.94.....	22 56 24.05	−31 33 56.0	330.53	−159.86	6.48	Gl 879	CD −32°17321	...	...	HHH
130.08.....	22 57 39.05	−29 37 20.1	329.22	−164.22	1.17	Gl 881	CD −30°19370	...	...	HHH
129.54.....	17 25 45.23	+02 06 41.1	−580.47	−1184.81	7.54	Gl 673	BD +02°3312	G019-024	...	HHH
129.40A.....	05 02 28.42	−21 15 23.9	−141.55	−221.74	8.31	Gl 185A	BD −21°1051	...	...	YHH
129.40B.....	...	...	...	...	...	Gl 185B	...	...	9.5	YH
128.93.....	18 36 56.34	+38 47 01.3	201.02	287.46	0.03	Gl 721	BD +38°3238	...	...	HHH
128.80.....	06 59 32.00	+19 19 55.4	835.4	−895.9	14.83	GJ 1093	...	G109-035	...	YYY
128.28.....	18 05 07.58	−03 01 52.7	570.14	−332.59	9.37	Gl 701	BD −03°4233	G020-022	...	HHH
127.99.....	10 12 17.67	−03 44 44.4	−152.93	−242.90	9.26	Gl 382	BD −03°2870	G053-029	...	HHH
126.00.....	13 31 46.70	+29 16 36.0	−227.7	−159.5	11.95	2128	...	G165-008	...	GCC
125.62.....	20 30 32.05	+65 26 58.4	443.25	284.06	10.54	Gl 793	...	G262-015	...	HHH
125.00.....	05 56 23.69	+05 20 46.9	−479.4	−940.9	14.11	GJ 1087	...	G099-047	...	YYY

Note.—The coordinates are given in the J2000.00 equinox and epoch, meaning that they include the proper motion and precession. Units of right ascension are hours, minutes, and seconds, and units of declination are degrees, arcminutes, and arcseconds. Source codes: (G) Reid et al. 1995; (C) CNS3; (H) *Hipparcos*; (Y) Yale. The three characters correspond to parallax, position, and V-band magnitude, respectively, and are meant to indicate where the listed value comes from; (D) if there are only two codes, there is no V magnitude. "SMA" means semimajor axis and is derived from the projected separation, if the companion is visibly detected, or the radial velocity orbital solution (Reid & Gizis 1997). Positions for companions are only given if grossly different from the primary star's position or if needed for identification purposes (i.e., to establish which star the companion is closest to in a multiple star system).

with $M_V < 11$ all the way out to 10 pc, although the majority of the incompleteness is in the far less studied southern sky ($\delta < -35°$). Their computation involves taking the densities of stars of different absolute magnitudes in the 5 pc volume in the CNS3 (widely used as a benchmark for complete stellar samples) and multiplying by the ratio of the volumes due to increasing the radius of the sample. The 5 pc sample in the CNS3 contains 53 stars with $\delta > -35°$. This implies that there should be another $3.096(53 \pm 7.3) = 164 \pm 23$ stars between 5 and 8 pc. However, there are only 110 such stars known. Since we surveyed 163 stars but expect those to be drawn from a population of 217 ± 30, we estimate that our catalog is complete to approximately 75% (assuming the stellar densities within 5 pc are correct). Any incompleteness is most likely among the very faintest stars (white dwarfs and late M dwarfs), because they are less likely to have been measured and studied in depth in large-scale stellar surveys. In addition, many of the nearby stars were found through large-scale proper-motion surveys. Some stars may therefore be missing from the nearby star sample because they have very small proper motions.

Reid & Gizis (1997) argue that the CNS3 is complete to $M_V < 14$ for $\delta > -30°$ within 10 pc. $M_V = 14$ corresponds to the spectral type M4.5. These considerations permit us to conclude that our sample is complete at least to spectral type M5, and possibly even fainter. We conservatively claim that the sample is 75% complete and believe that the

missing stars are all later than M5 in spectral type.

3. OBSERVATIONS

In pursuit of our goal to image and study brown dwarf companions of stars in our sample, we conducted observations of 107 of the 111 star systems (96% of the sample) in optical and near-infrared wavelengths. The observations employed two different imaging instruments, the AOC attached to the Palomar 60 inch telescope and the Cassegrain Infrared Camera fitted to the Palomar 200 inch (5 m) Hale Telescope.

3.1. *Common Proper Motion*

We imaged each of the stars at least twice in order to discern faint objects within 30″ of each star that display the same proper motion as the stars themselves. Our decision to use the common proper motion criterion was motivated by the plethora of models of brown dwarfs at the time the survey began. These models painted often-conflicting depictions of the colors or spectra that brown dwarfs ought to exhibit (see Burrows & Liebert 1993 for a comprehensive review of the state of these models at about the time that our survey began). We decided that instead of relying upon one of the models and designing a survey that looked for colors that such a model predicted, we would use a more basic physical argument for finding cool companions.

The technique we employ here is explained through example in Figure 1. This figure shows four z-band coronagraphic images of the star Gl 105A (138.72AC). The top two images are magnified portions of the region immediately around the star. These two images were taken a year apart and show a faint second object with the same proper motion. The star moves 2.″2 yr^{-1}, permitting extremely easy discrimination between common proper motion companions and background stars. This is demonstrated in the bottom two images, which are larger portions of the same images. In these two, one can clearly see that the two stars to the west do not share the proper motion of the star. We reported this common proper motion companion in Golimowski et al. (1995).

The error in the measurement of the centroid of a stellar image on a CCD is approximately the angular size of the image divided by the signal-to-noise ratio. (There is a correction factor if the pixel size is much smaller than the image size, but this amounts to a 0.6% correction in this survey. This is because we require every star to be imaged in 1″ seeing or better.) In our survey, we combine n measurements of each star to improve upon this standard as astrometric limit. The effective signal-to-noise ratio of the combined measurement is improved by the factor $n^{1/2}$. At each epoch we have at least two images. With at least two epochs per star, the value of n for most stars is greater than 4. The average value of n for all the stars in the survey with other

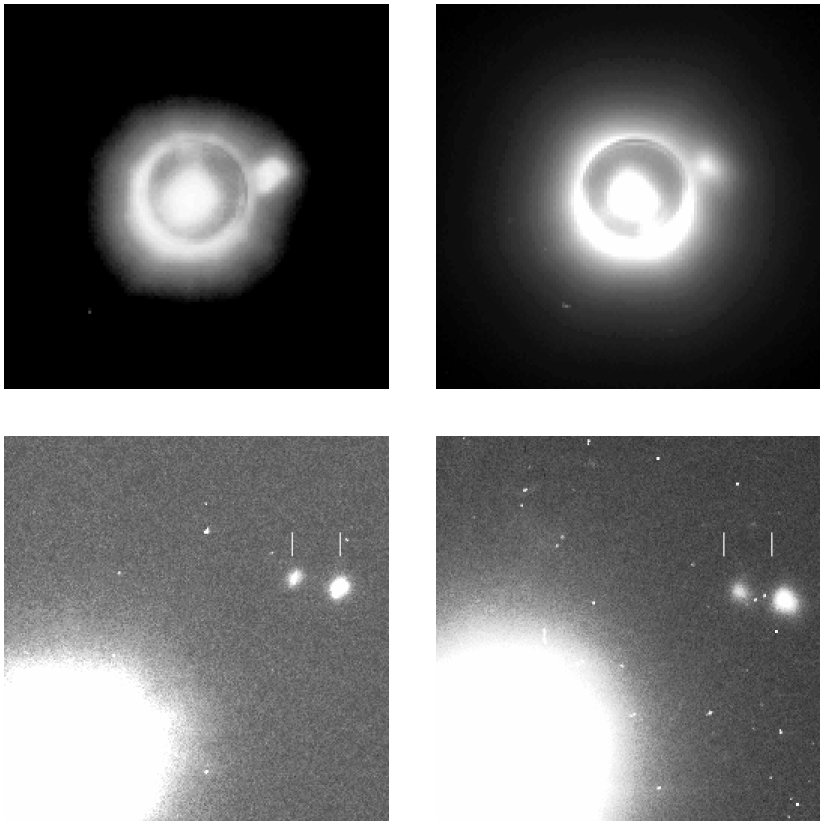

FIG. 1.—Images of Gl 105AC (138.72AC). The top two panels are magnified portions of the bottom panels. These images were taken in the z band in 1994 October (*left*) and 1995 October (*right*). North is up and east is to the left. The star has moved over 2.″2 between these two epochs, yet the fainter object maintains the same offset from the star in the top panels. This makes it a common proper motion companion. The seeing was better than 0.″6 in the images, and the astigmatism (which has since been fixed) of the 60 inch telescope is apparent. The pixel size is 0.″117. The top images measure 16″ on a side. The bottom images are 40″ on a side. The two white tick marks in the bottom left panel serve to mark the positions of the two field stars in 1994. In the bottom right panel they are placed in the same location to clearly show that the field stars have moved relative to the central star (which is placed in the same location in the two panels).

point sources in the field of view is 8. This means that the average centroid error for sources detected at the 5 σ level is 0.″07. All the stars in our sample exhibit proper motions greater than 0.″07 yr^{-1}. Thus, we are capable of discerning background objects from common proper motion companions with these observations. In most cases, the proper motions are actually substantially larger than 0.″07 yr^{-1} and the requirement on the astrometric errors is far less stringent than 0.″07.

3.2. *Optical Observations*

Optical coronagraphic images of the survey stars were obtained during 25 separate observing runs on the Palomar 60 inch telescope between 1992 September and 1999 April. These images were obtained with a Tektronix 1024 × 1024 pixel CCD camera binned in a 2 × 2 pattern (0.″117 $pixel^{-1}$) attached to the back end of the AOC. This device consists of a standard Lyot coronagraph (Lyot 1939) fitted behind a tip-tilt mirror, which uses the occulted star as a guide star. The tip-tilt correction provides substantial gains in image resolution on the Palomar 60 inch telescope, because there the majority of the atmospheric disruption of the stellar wave front resides in tip-tilt energy or, equivalently, image motion. We routinely obtained images with resolutions of 0.″7, and on six of the observing runs we obtained images at 0.″45 resolution. The images were taken through the Gunn r and z filters, with additional images taken through the i band if a companion was found. In almost all cases the CCD was exposed for 1000 s. However, for the stars whose magnitude is $V < 6$, we were forced to take shorter exposures and to sum these to produce a final image with a 1000 s exposure time. The AOC on the 60 inch telescope was incapable of guiding on stars fainter than $V \sim 13.5$. For this reason, we were unable to observe 13 of the sample stars with the AOC. We had to rely upon the infrared observations of these stars to discern companions. These stars are indicated by the words "too faint" in Table 2.

The AOC's focal-plane aluminum occulting stop is uniformly translucent in the r and z bands. This permits an accurate measurement of the position of the star in the CCD image. (Without the transparent stop, pinpointing the star would have been impossible because the pupil-plane stop eliminates the diffraction spikes of the star.) We used coronagraphic stops 4.″2 in diameter for most observations, except in the case of the brightest stars, where an 8.″4 diameter stop was used. We claim no sensitivity to faint companions under the stops. However, equal-brightness binaries were sometimes resolved under the masks (see, e.g., Fig. 10 below).

If a set of r- and z-band images failed to reveal any sources in the field of view other than the star, we would not reobserve the star. Table 2 lists the dates of all the observations of each star in the sample. In all cases we attempted to acquire images with seeing better than 1.″0. Seeing worse than this strongly degraded our sensitivity (§ 4). In all cases we were able to obtain such images at least once for each of the stars observed, and at least twice for those stars with possible companions (i.e., with any other point source in the field of view).

Data reduction involved the subtraction of a bias frame from each of the science images, division by a flat-field image obtained using the 60 inch dome and a flat-field lamp, and the removal of cosmic rays (easy to identify in these images because of the very small plate scale). The images were then inspected by eye. In most cases, this was sufficient to ascertain whether common proper motion companions were present. However, for the stars whose proper motions are small, additional work was required to distinguish field stars from common proper motion objects. Because the central occulting mask of the coronagraph was somewhat transparent, we were able to centroid the light of the survey star to ascertain its position in the images. Simple centroiding of the other point sources yielded pixel locations as well. These were converted into angular separations in arcseconds by using the observing run's plate scale and detector orientation. These were determined with the astrometric calibrator fields, as explained in § 3.4.

3.3. *Infrared Observations*

Direct infrared images of each of the sample stars were obtained with the D78 Cassegrain Infrared Camera on the Palomar 200 inch telescope during 15 observing runs between 1995 May and 1999 March. We allowed the stars to saturate the central part of the 256 × 256 InSb array (0.″125 $pixel^{-1}$). The field of view in these images was approximately 32″. Our imaging technique entailed the use of the J and K filters with two types of exposure through each filter. The first type involved a total of five co-adds of 1 s exposure time. These images were meant to reveal close binaries with a dynamic range on the order of 5 to 8 mag (depending on the seeing). The second type of exposure used five co-adds of 10 s. These exposures were designed to detect fainter companions outside of a 3″ radius from the star. In each case, a sky frame was taken immediately after the data image was acquired. The sky frame was taken in the same manner as the data image, but with the telescope pointed 50″ to the north or east. In some cases, we changed this distance because of the presence of a rather bright source in the sky frame.

As with the optical observations, if no objects other than the star appeared, we would not observe the star a second time. In addition, the seeing requirement of $\leq 1.''0$ for the infrared observations was identical to that for the optical images (see above).

The data reduction for the infrared images involved the subtraction of the sky frame from the "on source" frame. Subsequent division by a flat field (acquired from the twilight sky during each observing run) permitted a more detailed examination of the images. As with the optical data, visual inspection of the images was usually enough to discern common proper motion companions. In cases where more accurate measurements were necessary, we needed to pinpoint the location of the survey star. This could not be done through centroiding, because all the stars' images were saturated. Fortunately, we could use the diffraction spikes in the infrared images (absent in the optical images because of the pupil-plane apodizing mask in the coronagraph). By fitting the unsaturated parts of the two diffraction spikes with perpendicular lines, we were able to localize the star with an accuracy of better than a third of a pixel. (We confirmed this through short unsaturated exposures of some of the fainter stars in the sample while the telescope guided on a field star. The low-frequency tip-tilt system on the f/70 secondary mirror of the 200 inch telescope guides with an accuracy of better than 0.″03 over 20 minutes.) This stellar position on the detector was then used, along with centroids of the light from putative companions, to compute offsets between the objects. These were

TABLE 2

LIST OF OBSERVATIONS OF THE 8 pc SAMPLE

Parallax (mas)	V (mag)	Dates of AOC Observations	Dates of Infrared Observations
549.01.....	9.54	1992 Sep, 1994 Apr	1996 Aug, 1997 Jul
419.10.....	13.46	1997 Feb, 1997 Apr	1996 Dec
392.40.....	7.49	1994 Apr	1996 Dec
379.21.....	−1.44	1996 Nov, 1998 Jan	1996 Oct
373.70.....	12.52	1994 Oct, 1995b Oct	1996 Aug
336.48.....	10.37	1995 Jun, 1995 Aug, 1995a Oct, 1996 Jun	1996 Aug, 1997 Jul
316.00.....	12.27	1992 Sep, 1995 Aug, 1995a Oct, 1995b Oct, 1997 Sep	1996 Aug, 1997 Jul
310.75.....	3.72	1995b Oct	1996 Aug, 1997 Nov
299.58.....	11.12	1993 Jan, 1996 Feb, 1997 Apr	1996 Dec
289.50.....	12.32	1995 Jun, 1995 Aug, 1997 Sep	1995 Sep, 1996 Aug
287.13.....	5.20	1995b Oct, 1996 Aug	1996 Aug
285.93.....	0.40	1995 Feb, 1996 Nov, 1998 Jan	1997 Nov
280.28.....	8.94	1992 Jun, 1996 Aug, 1997 Apr	1996 Aug, 1997 Jul
280.27.....	8.09	1995b Oct, 1997 Sep	1996 Aug, 1996 Dec, 1997 Aug
275.80.....	14.81	Too faint	1995 Nov, 1996 Dec
274.17.....	3.49	1995b Oct, 1996 Nov	1995 Nov, 1996 Aug, 1997 Aug
269.05.....	12.10	1995 Aug, 1996 Nov, 1997 Sep	1995 Sep, 1996 Aug
263.26.....	9.84	1995 Feb, 1997 Feb	1996 Dec, 1997 Nov
249.52.....	9.59	1995b Oct, 1996 Aug	1995 Nov, 1997 Jul
242.89.....	11.12	1995 Feb, 1995 Dec, 1996 Nov	1995 Nov, 1996 Oct, 1996 Dec
235.24.....	11.72	...	1999 Mar
234.51.....	10.10	1994 Apr, 1997 Apr, 1997 Jun	1996 Aug, 1997 Jul
227.90.....	12.44	1993 Jan, 1996 Feb, 1997 Apr	1996 Dec
227.45.....	12.16	...	1999 Mar
226.95.....	12.37	1992 Sep, 1995 Aug	1996 Aug, 1996 Dec
224.80.....	12.26	1995 Aug, 1995a Oct, 1995b Oct, 1997 Sep	1995 Sep, 1995 Nov, 1996 Aug, 1996 Oct
224.00.....	10.89	1995 Feb, 1995 Nov, 1996 Nov, 1998 Jan, 1998 Mar	1996 Dec, 1998 Mar, 1998 Dec
221.80.....	12.07	...	1999 Mar
220.85.....	9.15	1995 Jun, 1995 Aug, 1997 Sep	1996 Aug, 1997 Jul
220.30.....	15.60	Too faint	1996 Feb, 1996 Dec
220.20.....	13.41	1992 Sep, 1997 Aug	1995 Nov, 1996 Aug, 1997 Jul, 1997 Aug
213.00.....	13.74	1997 Sep	1996 Oct
212.69.....	10.16	1993 Oct, 1994 Oct, 1995 Aug, 1997 Sep	1996 Aug, 1997 Jul
206.94.....	8.82	1994 Apr	1996 Feb, 1996 Dec
205.22.....	6.60	1993 Jan, 1997 Apr	1996 Feb
204.60.....	9.40	1994 Apr, 1995 Feb, 1995 Dec	1995 Dec, 1996 Dec
202.69.....	11.39	...	1999 Mar
198.24.....	4.43	1996 Feb, 1996 Nov, 1997 Sep	1996 Oct, 1996 Dec
198.00.....	10.06	...	...
196.62.....	4.03	1996 Aug, 1997 Aug, 1997 Sep	1996 Aug
194.44.....	0.76	1995b Oct	1996 Aug
191.86.....	11.49	1996 Nov, 1997 Sep	1996 Dec, 1997 Aug
191.20.....	14.06	Too faint	1996 Dec, 1998 Mar
186.20.....	11.33	1995 Dec, 1996 Nov, 1998 Jan	1996 Oct, 1996 Dec, 1997 Nov
185.48.....	10.80	1997 Feb	1996 Dec
184.13.....	8.46	1993 Jan, 1994 Apr, 1997 Apr	1996 Dec, 1997 Jul
182.15.....	11.41	...	...
181.36.....	10.82	1996 Nov, 1997 Sep	1996 Oct, 1996 Dec
181.32.....	9.89	1996 Nov, 1998 Jan	1996 Oct
177.46.....	11.64	1997 Feb, 1997 Apr, 1998 Jan	1996 Dec
175.72.....	7.97	1996 Nov, 1998 Jan	1996 Dec
174.23.....	9.02	1996 Aug, 1997 Apr	1996 Aug, 1997 Jul
173.41.....	4.67	1996 Aug	1996 Aug
173.19.....	8.15	1994 Oct, 1995 Feb, 1995a Oct	1995 Sep, 1995 Nov, 1996 Oct, 1996 Dec
172.78.....	11.56	1996 Nov, 1998 Jan	1996 Oct, 1996 Dec, 1997 Nov
170.26.....	9.12	1992 Sep, 1996 Jun	1996 Aug, 1997 Jul
169.90.....	12.10	1996 Nov, 1998 Jan	1996 Dec, 1997 Nov
169.32.....	5.72	1997 Apr	1997 Jul
168.59.....	11.19	1995 Feb, 1995 Nov, 1996 Nov, 1998 Jan	1995 Dec, 1996 Dec, 1997 Nov
167.99.....	3.46	1996 Nov, 1997 Aug	1996 Oct, 1997 Aug
167.51.....	8.98	1992 Sep, 1993 Oct, 1996 Nov, 1997 Sep	1996 Aug, 1997 Aug
167.08.....	4.33	1997 Apr, 1997 Sep	1997 Jul, 1998 Jun
164.70.....	14.15	Too faint	1998 Mar
163.51.....	11.32	1993 Jun, 1997 Apr	1997 Jul
163.00.....	12.1	1996 Nov	1996 Oct, 1996 Dec

TABLE 2—*Continued*

Parallax (mas)	*V* (mag)	Dates of AOC Observations	Dates of Infrared Observations
162.50.....	5.85	1997 Apr	1996 Dec
162.00.....	13.22	1998 Jan	1995 Dec, 1996 Dec
161.77.....	11.39	...	1999 Mar
161.59.....	7.64	1996 Nov	1996 Dec
160.06.....	10.05	1995a Oct, 1997 Sep	1995 Nov, 1996 Aug, 1997 Jul
159.52.....	10.57	1993 Jun, 1994 Apr	1997 Jul, 1998 Mar
158.17.....	9.31	1994 Apr, 1997 Sep	1996 Aug, 1997 Jul
157.24.....	11.65	1994 Oct, 1995 Nov	1995 Nov, 1996 Oct
156.30.....	17.05	Too faint	1998 Mar, 1998 Jun
156.00.....	12.58	1997 Apr, 1997 Jun	1996 Dec
155.00.....	14.45	Too faint	1996 Oct, 1996 Dec, 1998 Mar
153.24.....	5.57	1996 Aug, 1996 Nov, 1997 Aug	1996 Aug, 1997 Jul
152.90.....	13.79	1997 Apr, 1998 Jan	1996 Feb, 1996 Dec
151.93.....	10.13	1997 Apr	1997 Jul
150.96.....	10.03	1997 Feb, 1997 Apr, 1998 Jan	1996 Dec
149.26.....	4.54	1997 Apr	1997 Jul
148.29.....	10.33	1994 Oct, 1996 Aug	1996 Aug
146.30.....	12.83	1996 Nov, 1997 Apr	1996 Dec, 1997 Nov, 1998 Mar
145.27.....	8.68	1996 Nov, 1997 Sep, 1998 Jan	1996 Oct, 1997 Jul
143.45.....	5.91	1997 Aug, 1997 Sep	1997 Jul, 1998 Jun
141.95.....	8.55	1993 Jun, 1996 Jun, 1996 Nov	1996 Aug, 1997 Jul
138.72.....	5.79	1993 Oct, 1994 Oct, 1995 Aug, 1995a Oct	1995 Sep, 1996 Oct, 1996 Dec, 1997 Aug, 1998 Dec
138.30.....	14.69	Too faint	1996 Oct, 1997 Oct
138.29.....	9.65	1994 Apr, 1995 Feb, 1996 Nov, 1997 Apr, 1998 Jan, 1998 Mar	1996 Dec
137.84.....	11.77	...	1997 Jul
137.50.....	13.46	Too faint	1997 Jul
135.30.....	15.42	Too faint	1995 Sep, 1996 Aug
134.40.....	13.25	1997 Sep	1997 Jul
134.04.....	5.74	1993 Oct, 1996 Nov	1996 Aug, 1996 Dec, 1997 Aug
133.91.....	5.24	1993 Oct, 1996 Aug, 1997 Sep	1996 Aug
132.60.....	13.64	Too faint	1997 Jul, 1998 Jun
132.42.....	10.55	1995b Oct, 1997 Feb	1996 Aug
132.40.....	5.17	1996 Aug, 1996 Nov, 1997 Aug	1996 Dec
132.10.....	11.71	1996 Nov, 1998 Jan	1996 Oct, 1996 Dec, 1997 Nov
131.12.....	9.05	1997 Apr	1996 Dec
130.94.....	6.48	1997 Aug	1996 Oct, 1997 Jul
130.08.....	1.17	1996 Nov, 1997 Sep	1996 Oct
129.54.....	7.54	1994 Apr, 1997 Apr	1996 Aug, 1997 Jul
129.40.....	8.31	1996 Nov, 1998 Jan	1996 Oct, 1996 Dec, 1997 Nov, 1998 Mar, 1999 Mar
128.93.....	0.03	1997 Sep	1997 Jul
128.80.....	14.83	Too faint	1996 Oct, 1996 Dec, 1997 Nov
128.28.....	9.37	1997 Aug, 1997 Sep	1997 Jul, 1998 Mar, 1998 Jun
127.99.....	9.26	...	...
126.00.....	11.95	1995 Jun, 1997 Apr, 1997 Jun	1996 Feb, 1996 Dec, 1997 Jul
125.62.....	10.54	...	1999 Mar
125.00.....	14.11	Too faint	1996 Oct, 1997 Nov

converted into angular offsets in arcseconds by using the plate scale, as described in § 3.4.

3.4. *Astrometric Calibration*

In order to obtain accurate astrometric measurements of the offsets between the central star and its putative companions, we made observations of calibration fields during each observing run. These fields contained 6 to 10 stars whose relative positions are known within a few milliarcseconds. We used these fields to determine that the astrometric distortion on the face of the CCD chip used in the AOC observations was smaller than 0.″01 over the whole chip. In the infrared observations, the distortion is almost a full pixel near the edges of the array. This distortion is constant with time. Because we centered the stars in the same position on the infrared array at each observing run, the comparison of astrometric measurements is valid despite this image distortion. We did not use relative astrometry measured on the infrared images in conjunction with other measurements made on the AOC images. For these reasons, we applied no astrometric distortion correction in our measurements of relative offsets between stars.

For all of the infrared observing runs, the data were taken with the Cassegrain ring angle precisely set to place north up and east left on the array. This prevented complications in astrometric measurements that would arise from using arbitrary position angles of the array with respect to the cardinal directions.

For every AOC observing run, we would observe whichever of the three astrometric calibration fields (listed in Tables 3–5) was visible. In each case, we would place the star shown in the center of each of Figures 2–4 in the center

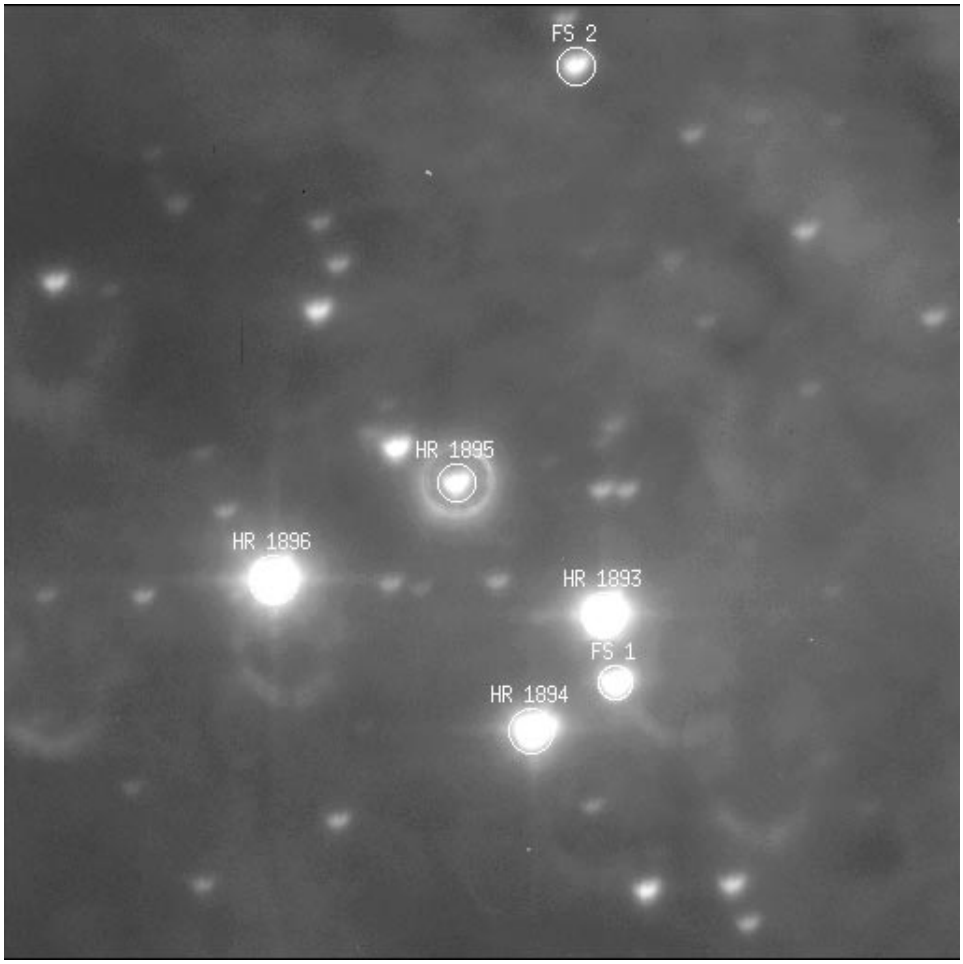

FIG. 2.—Trapezium astrometric calibration field. The stars marked with circles and numbers are the stars listed in Table 3 and are the ones used to conduct the calibration. The image measures 1′ on a side. North is down and east is to the left.

TABLE 3

TRAPEZIUM CALIBRATION FIELD

Star Name	R.A. (J2000.00)	Decl. (J2000.00)
HR 1895.....	05 35 16.462	−05 23 23.03
HR 1893.....	05 35 15.821	−05 23 14.45
HR 1894.....	05 35 16.129	−05 23 06.96
HR 1896.....	05 35 17.248	−05 23 16.69
FS 1	05 35 15.768	−05 23 10.06
FS 2	05 35 15.953	−05 23 49.99

NOTE.—HR 1895 is the central, occulted star in the image. Position data are from McCaughrean & Stauffer 1994.

TABLE 4

M5 CALIBRATION FIELD

Star Name	R.A. (B1950.00)	Decl. (B1950.00)
93	15 16 01.70	+02 11 31.7
94	15 16 03.14	+02 12 00.0
95	15 16 02.46	+02 12 09.6
96	15 16 04.36	+02 12 09.7
97	15 16 05.05	+02 12 20.3

NOTE.—Positions and numbering scheme are from Cudworth 1979. Star 93 is occulted and centered in the image.

of the field of view. This star was used for guiding and rapid tip-tilt image motion compensation. From the images—500 s *r*-band exposures—we were able to determine precisely the plate scale and the rotation of the CCD on the plane of the sky. We found that the plate scale was extremely stable in both instruments (despite the fact that the CCD camera used on the AOC was taken apart and reassembled twice between the starting and ending dates of the survey). The accurate positions of the stars in these fields are from Cudworth (1979) for M5, Cudworth (1976) for M15, and McCaughrean & Stauffer (1994) for the Trapezium.

TABLE 5

M15 CALIBRATION FIELD

Star Name	R.A. (B1950.00)	Decl. (B1950.00)
275	21 27 22.82	+11 55 33.6
277	21 27 24.40	+11 55 15.3
278	21 27 24.83	+11 55 30.2
279	21 27 25.93	+11 55 30.0
280	21 27 26.80	+11 55 43.5
281	21 27 25.24	+11 55 51.0
282	21 27 24.09	+11 55 52.1

NOTE.—Positions and numbering scheme are from Cudworth 1976. Star 278 is occulted and centered in the image.

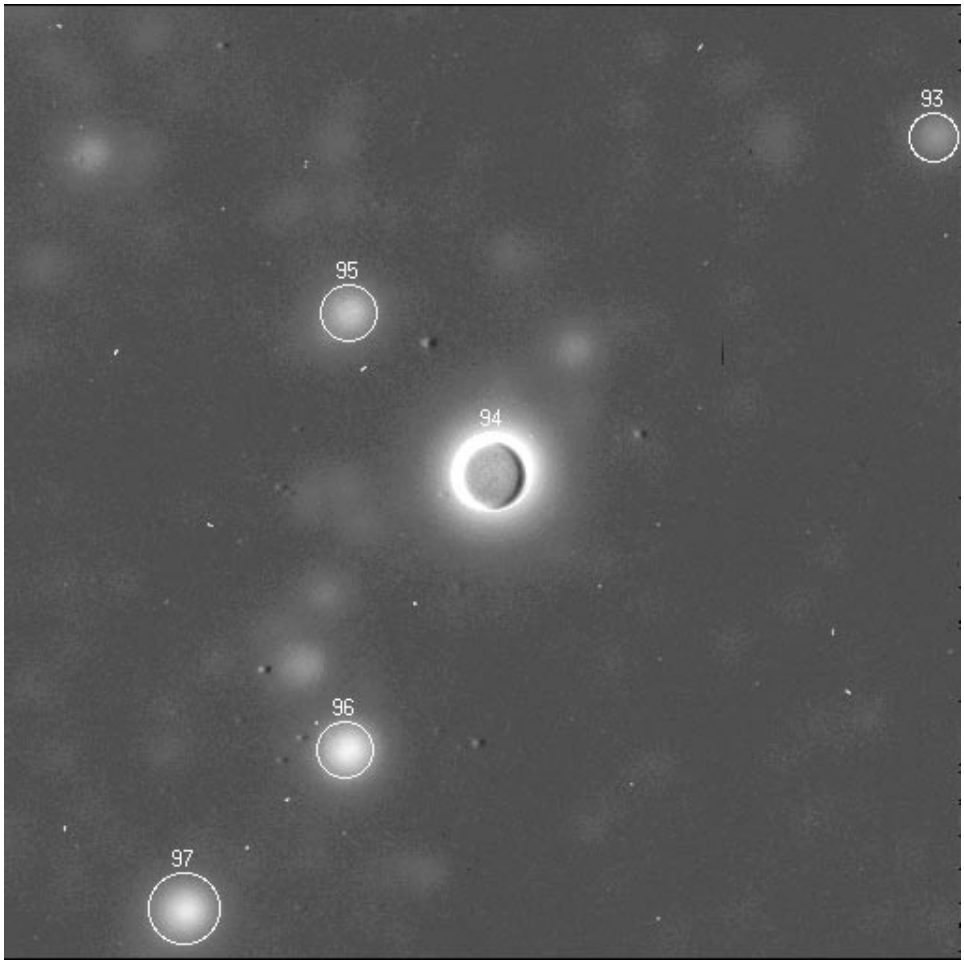

FIG. 3.—M5 astrometric calibration field. The stars marked with circles and numbers are the stars listed in Table 4 and are the ones used to conduct the calibration. The images measure 1′ on a side. North is to the left and east is down.

Figures 2, 3, and 4 show each of the three calibration fields, and Tables 3, 4, and 5 give the positions of the stars used for the astrometric calibration.

4. DETECTION LIMITS FOR EACH STAR

Typically in imaging surveys, assessing the sensitivity of the images and the survey as a whole simply involves a determination of the limiting magnitudes of the images. However, in this case the problem is somewhat more complicated.

The presence of the bright star in our images means that over much of the field of view, the sensitivity is limited by the light of the star and not the sky background (or read noise, as was the case for speckle interferometric surveys of these stars; Henry & McCarthy 1990). However, this survey extends into uncharted parameter space because the coronagraphic technique suppresses a substantial portion of the starlight. The image shown in Figure 5 illustrates this with the Gl 105AC system.

We have measured the detection limits for each star in the survey as a function of angular separation from the central star. To do this, we took images of each star with 1.″0 seeing or better—the acquisition of such images was a survey requirement (§ 3)—and inserted artificial point sources at an array of separations from the star. These artificial point sources were generated with appropriate Poisson noise statistics and angular sizes to match the seeing conditions. The magnitudes of these artificial stars (calibrated to the photometric standards used during the relevant observing run) were set so that each artificial star was just visible to the eye. From these magnitudes, the sensitivity curve is derived. An example of this is shown in Figure 6.

From this procedure, we had a measurement of the faintest source visible at a set of about 10 to 15 radii from the star. Using a spline interpolation between these points, we derived the magnitude limit for r, z, and J as a function of radius measured from the star. In each band, we have individual curves of this nature for each central star in the survey. These curves are summarized in Figures 7, 8, and 9, where we have displayed representative curves for different star brightnesses in each bandpass.

There are several important effects documented by the curves in Figures 7–9. The most obvious is that the z-band imaging is the most sensitive, achieving a maximum dynamic range of 15.5 mag at 10″ while, in addition, even the brightest companions can be imaged inside the 5″ radius. In comparison, the J band has no sensitivity at the 5″ radius for the bright stars and only achieves a maximum dynamic range of 13 mag. What is even more important is the large, slowly eroding wing of the point-spread function in the J band. The r and z bands do not have nearly as much of this broad wing, primarily because of the pupil-

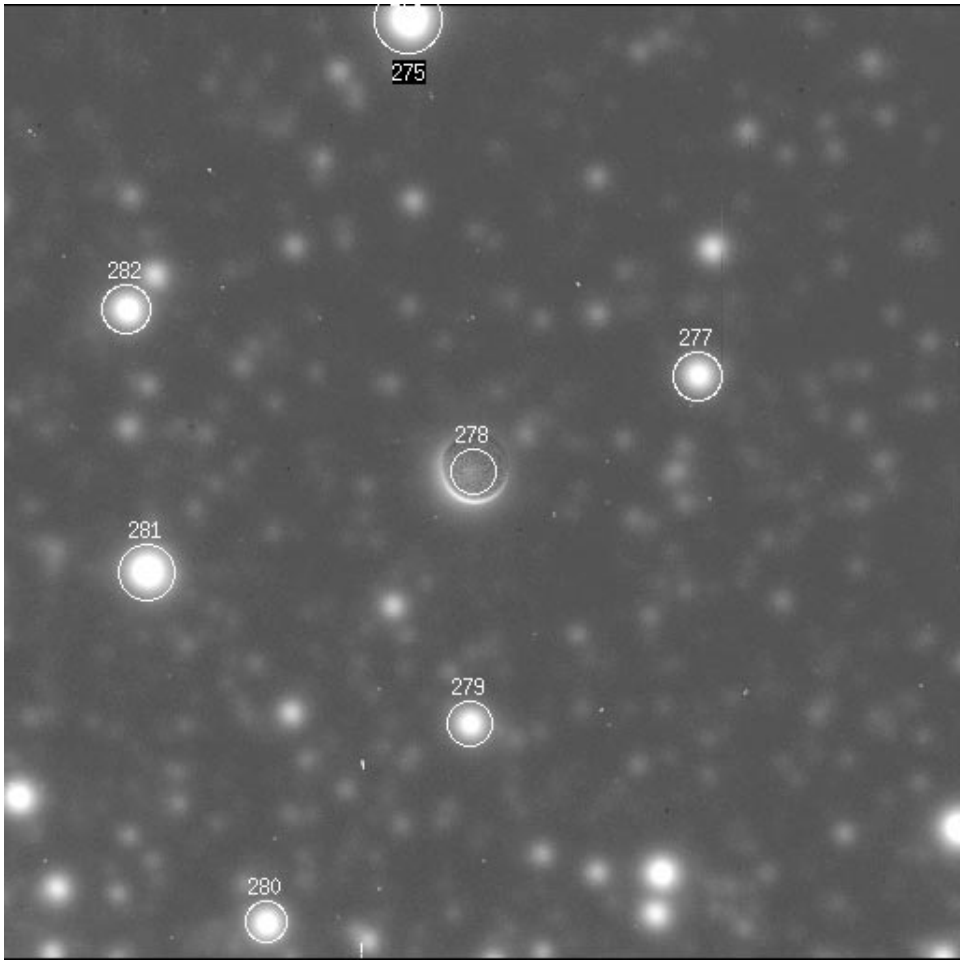

FIG. 4.—M15 astrometric calibration field. The stars marked with circles and numbers are the stars listed in Table 5 and are the ones used to conduct the calibration. The image measures 1′. North is to the left and east is down.

plane stop in the coronagraph. This stop is designed specifically to depress the wings of the stellar point-spread function.

5. DETECTION LIMITS FOR THE SURVEY

From the observational point of view, the curves in Figures 7–9 are the ultimate measure of the sensitivity of our survey. These curves parameterize the sensitivity for every star in the sample. However, it is of paramount importance to convert the information in Figures 7–9 into statements about the survey as a whole and in terms of physical, not observational, parameters. For example, can we safely claim with these data that for all the stars within 8 pc we would have detected *any* unknown stellar companions in orbits between 3 and 200 AU?

To address this issue, we use the curves found in the previous section to determine the number of surveyed stars for which we could have detected a companion of a given magnitude at a given separation. This information is expressed in terms of the fraction (or percentage) of the total number of stars imaged as a function of magnitude and physical separation in AU. To do this, we systematically went through the catalog of stars. For each star, we took the relevant sensitivity curve, as derived in the previous section, and converted the magnitude scale into absolute magnitudes, using the parallax of the star. We also converted the angular scale into physical separation in AU by dividing by the parallax in arcseconds. Then we tested whether companions with a set of magnitudes in each band and a set of separations would be visible in our images. By doing this exercise for every star observed, we ended up with a tally of the number of stars, as a function of magnitude and separation, for which the analysis showed that a companion would be visible.

This analysis was done for each of the *r*, *z*, and *J* bands (the *K*-band sensitivity curves are essentially identical to the *J*-band curves, so we did not independently conduct this analysis for the *K* band). The results are shown in Tables 6, 7, and 8.

The drop-off in the survey sensitivity at large physical companion separations is due to the varying physical field of view caused by the distribution of parallaxes of the stars in the survey. In the *J* band there is no sensitivity outside of 120 AU, for example, because the field of view is 15″ and the minimum parallax is 125 mas.

We have divided Tables 6–8 horizontally at the approximate absolute magnitude of a 0.08 $M_{\odot}$ star. If the hydrogen-burning mass limit is 0.08 $M_{\odot}$, then all stellar companions must be brighter than the absolute magnitude indicated by the divider. Brown dwarfs can be brighter than this line if they are young, but objects below this line must be brown dwarfs and not stars. There are some indications

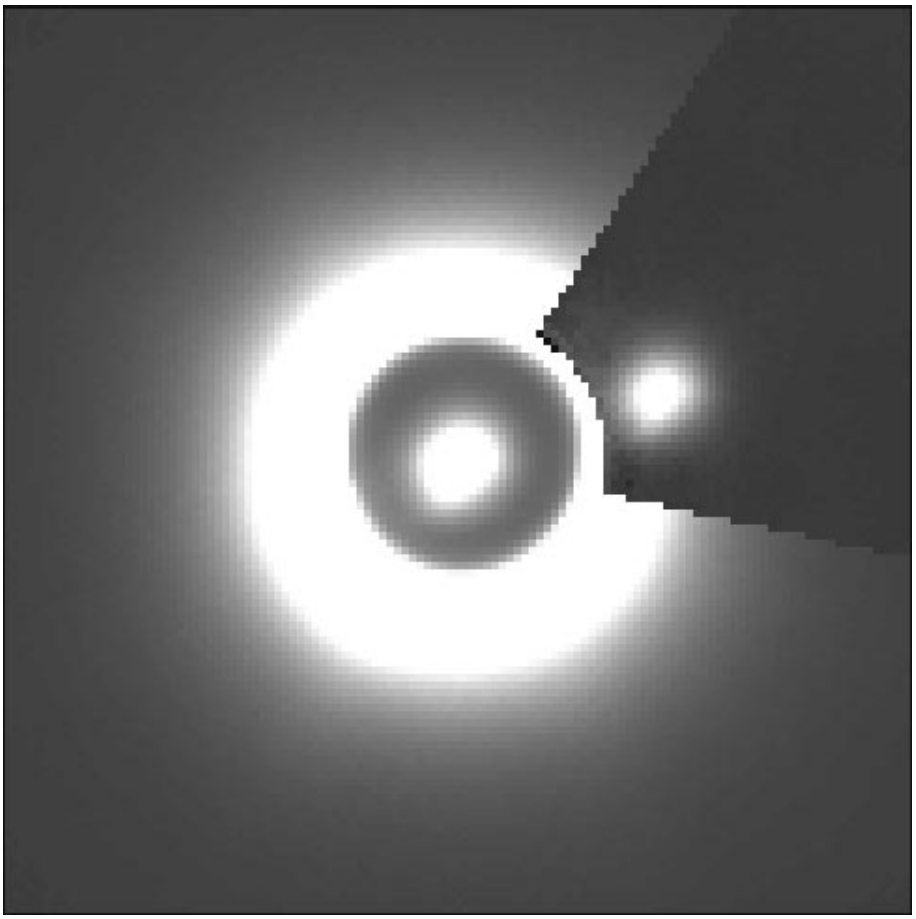

FIG. 5.—Image of Gl 105AC. This image, taken through the *i* band in 1993 October, shows only the inner 14.″5 × 14.″5 piece of the larger AOC image. North is up and east is to the left. The occulting mask (somewhat transparent) is 4.″3 in diameter and reveals the core of the star's seeing disk. Outside the occulted region, part of the seeing disk has been modeled and subtracted to make the companion stand out better. This is unnecessary in order to see the companion, however, as shown in Fig. 1. This image demonstrates the huge dynamic range possible with the AOC. Only 3.″3 from a star with $i = 7.03$ mag, we detected with ease a very low mass star with $i = 12.6$ mag with a signal-to-noise ratio of several thousand. We could have detected a companion at this separation in this image as faint as 18.5 mag, indicating a dynamic range of 11.5 mag at 3.″3. (From Golimowski et al. 1995.)

that the hydrogen-burning mass limit may not be 0.08 $M_\odot$. We refer the reader to Gizis et al. (2000) and references therein for observational evidence.

6. SENSITIVITY TO STELLAR COMPANIONS

We now extend the analysis from the previous section. Instead of discussing the survey sensitivity in terms of observational quantities, we relate those quantities to known properties of stars. This allows us to determine the ability of the survey to find stellar companions of the survey stars. A stellar companion at the minimum mass for hydrogen burning (0.08 $M_\odot$; Burrows et al. 1997) has absolute magnitudes of $M_r = 17.4$, $M_z = 14.9$, and $M_J = 11.5$. These magnitudes are determined by averaging the photometry of

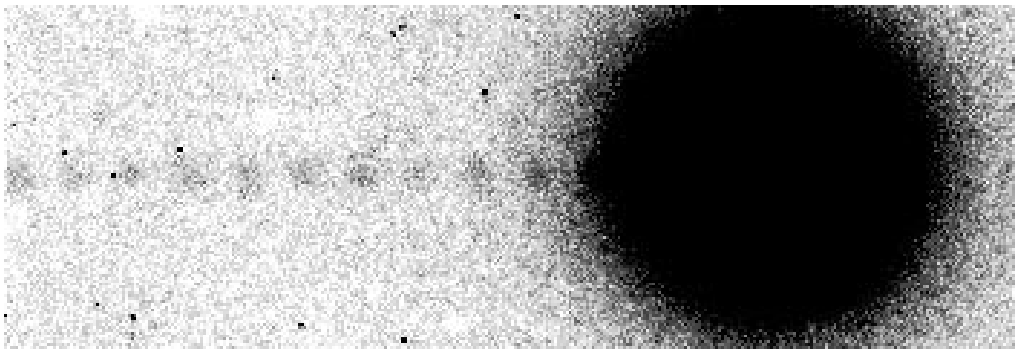

FIG. 6.—Example of the sensitivity-curve determination technique. The images shown are part of a *z*-band coronagraphic image of G192-013 (132.10). The artificial point sources are visible to the left of the star and are placed at regular intervals of 20 pixels. The gray-scale stretch shows the lowest light levels, permitting visibility of the large-separation artificial sources while excluding the sources close to the star. The image measures approximately 40″ × 10″. The sensitivity curve derived from this image is the lowest one in Fig. 8.

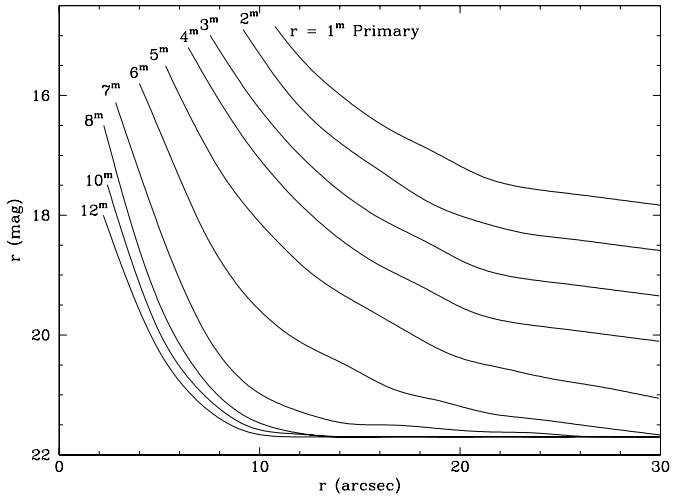

FIG. 7.—Sensitivity curves for the *r* band showing magnitude limit as a function of separation (in arcseconds) from the star for stellar magnitudes ranging from 1 to 12.

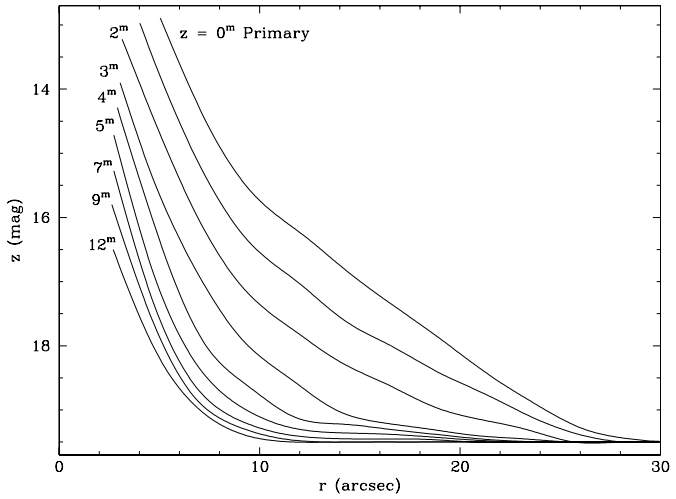

FIG. 8.—Same as Fig. 7, but for the *z* band for stellar magnitudes ranging from 0 to 12.

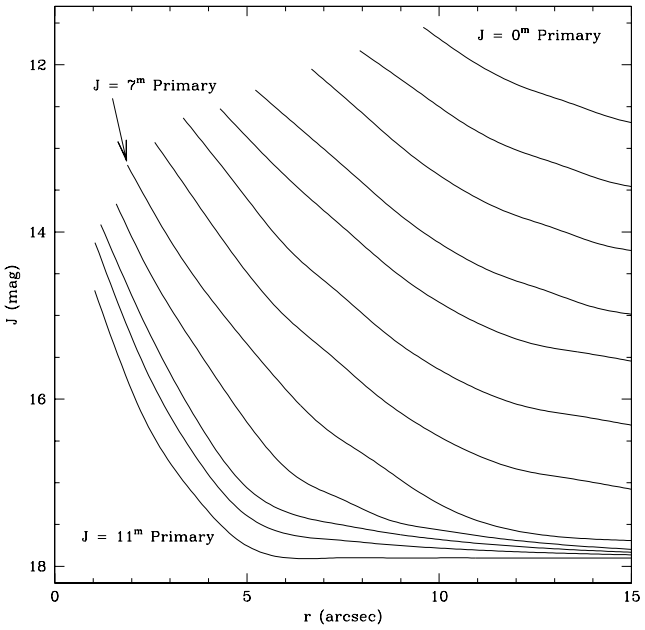

FIG. 9.—Same as Fig. 7, but for the *J* band for stellar magnitudes ranging from 0 to 11.

several of the objects known to be at the minimum stellar mass (Henry & McCarthy 1993). (It is important to note, however, that the exact location of the "hydrogen-burning mass limit" is not precisely known. For example, Gizis et al. 2000 suggest that some L dwarfs might be hydrogen burning and yet have masses below 0.08 $M_{\odot}$.) We now use these measurements to make a single table showing the sensitivity to a minimum mass star in each of the bandpasses. The result is shown in Table 9.

What this table demonstrates is that the combination of the infrared and optical imaging permits the detection of any stellar companion at separations greater than 10 AU. We note that for the smaller separations, the *J* band is most sensitive. The *z* band is more sensitive than the *J* band at the higher separations. This is primarily due to the drop in

TABLE 6

PERCENTAGE OF SURVEY STARS WITH OBSERVATIONS SENSITIVE TO COMPANIONS OF ALL *J* MAGNITUDES

	SEPARATION (AU)									
M_J	2.5	5	10	20	40	80	120	160	200	225
Stars										
9.9	1	31	97	99	98	60	2	0	0	0
10.9.....	1	31	97	99	98	60	2	0	0	0
Cool Brown Dwarfs										
11.9.....	1	31	97	99	98	60	2	0	0	0
12.9.....	1	31	97	95	94	59	2	0	0	0
13.9.....	1	26	81	90	83	59	2	0	0	0
14.9.....	0	5	46	80	80	56	2	0	0	0
15.9.....	0	4	28	66	73	48	2	0	0	0
16.9.....	0	1	5	33	65	45	2	0	0	0
17.9.....	0	0	0	4	25	15	1	0	0	0
18.9.....	0	0	0	0	0	0	0	0	0	0

NOTE.—M_J is the absolute magnitude in the *J* band.

TABLE 7

PERCENTAGE OF SURVEY STARS WITH OBSERVATIONS SENSITIVE TO COMPANIONS OF ALL z MAGNITUDES

	Separation (AU)									
M_z	2.5	5	10	20	40	80	120	160	200	225
					Stars					
11.5.....	0	1	29	100	100	97	84	60	26	13
12.5.....	0	1	29	100	100	97	84	60	26	13
13.5.....	0	1	26	83	99	97	84	60	26	13
14.5.....	0	1	25	75	99	97	84	60	26	13
					Cool Brown Dwarfs					
15.5.....	0	1	25	67	98	97	84	60	26	13
16.5.....	0	0	20	59	92	95	84	60	26	13
17.5.....	0	0	3	28	83	95	83	60	26	13
18.5.....	0	0	1	8	67	94	83	59	26	13
19.5.....	0	0	0	0	9	67	66	52	25	12
20.5.....	0	0	0	0	0	0	0	0	0	0

NOTE.—M_z is the absolute magnitude in the z band.

coverage at large separations in the J band (where the field of view is only 32″).

Indeed, we have detected six new stellar companions of these stars. These are described below.

7. NEW COMPANIONS

In the course of our observations, we have discovered or confirmed seven new companions of nearby stars. Three of these stars originally included in the 8 pc sample have been removed from the sample because of new and more accurate trigonometric parallaxes. The new companions belong to the following systems: Gl 105 (138.72), Giclas 089-032 (162.00), Gl 229 (173.19), Giclas 041-014 (224.00), LP 476-207, LP 771-095 (LTT 1445), and LHS 1885 (Giclas 250-031). Only Gl 229B is substellar. The last three in the list are no longer part of the 8 pc sample, which means that four of our new companions are in the 8 pc sample. Since Gl 105AC (Fig. 1) and Gl 229AB have been reported and

TABLE 8

PERCENTAGE OF SURVEY STARS WITH OBSERVATIONS SENSITIVE TO COMPANIONS OF ALL r MAGNITUDES

	Separation (AU)									
M_r	2.5	5	10	20	40	80	120	160	200	225
					Stars					
13.7.....	0	1	29	100	100	97	84	60	26	13
14.7.....	0	1	29	100	100	97	84	60	26	13
15.7.....	0	1	29	98	90	95	84	60	26	13
16.7.....	0	1	27	89	85	95	83	60	26	13
					Brown Dwarfs					
17.7.....	0	0	20	72	82	93	82	59	25	13
18.7.....	0	0	6	54	79	87	82	59	25	11
19.7.....	0	0	5	51	79	80	77	58	25	11
20.7.....	0	0	0	5	57	77	70	52	25	11
21.7.....	0	0	0	0	8	58	64	44	17	9
22.7.....	0	0	0	0	0	0	0	0	0	0

NOTE.—M_r is the absolute magnitude in the r band.

TABLE 9

PERCENTAGE OF SURVEY STARS WITH OBSERVATIONS IN J, z, AND r SENSITIVE TO 0.08 $M_\odot$ STELLAR COMPANIONS

	Separation (AU)									
BAND	2.5	5	10	20	40	80	120	160	200	225
J.....	1	31	97	99	98	60	2	0	0	0
z.....	0	1	25	72	98	97	84	60	26	13
r.....	0	1	27	89	82	95	83	59	26	13

described in detail elsewhere, we simply refer the reader to Golimowski et al. (1995) for Gl 105AC and Nakajima et al. (1995), Oppenheimer et al. (1995), Matthews et al. (1996), Golimowski et al. (1998), and Oppenheimer et al. (1998) for Gl 229AB. Below we describe the other companions.

7.1. *Giclas 089-032 (162.00)*

G089-032, with no trigonometric parallax measurement, is listed in the CNS3 with a photometric parallax of 162.00 mas and a spectral type of M5. The Palomar survey has resolved the star into a binary of equal magnitude. It was noted as a double source with 0.″7 separation in Henry et al. (1997), but they had no information to determine whether the two components were physically associated. In our coronagraphic images taken in 1998 January, we resolve the two components under the semitransparent focal-plane mask. The short infrared images also barely resolve the components. With images taken between 1995 December and 1998 January and the known proper motion of the star, 0.″354 yr^{-1}, we have ascertained that the two components exhibit the same proper motion and no measurable change in relative offset during this time span. Figure 10 shows two of our images. Our measured separation is 0.″73.

7.2. *Giclas 041-014 (224.00)*

G041-014 is a star with a photometric parallax of 224 mas. There is no trigonometric parallax measurement for this star. Reid & Gizis (1997) report that this object has a spectroscopic companion of approximately equal mass. Delfosse et al. (1999) have determined the orbit of this companion (with a period of 7.6 days). However, Delfosse et al. also claim to have resolved a third component of the system with adaptive optics images. They did not publish a confirmation of common proper motion for this object. We have determined that it is a physical companion. They determine a separation of 0.″62 and a difference of 0.5 mag at the K band. This star, which is listed in their Table 4 (as LHS 6158) as a binary, was included in our survey. We observed it eight times over the duration of this project. Only two of our observations were capable of resolving this putative companion. Both observations were with the AOC in extremely good seeing conditions, where the corrected image sizes were 0.″45 and 0.″50. We resolved the companion and measured offsets of 0.″47 in 1996 November and marginally resolved the companion at 0.″52 in 1998 March. (The standard errors discussed in § 3.4 apply to the 1996 November measurement. However, since we only marginally resolved the two components in 1998 March, we suggest that the error on that measurement is $\pm$0.″1.) Despite the marginal resolution in 1998 March, the expected change in relative offset of this star over this period of time is about 1″. Thus, if it were a background object we would have easily measured this large change in the offset. The magnitude difference in the z band is approximately 1.6. Figure 11 shows the 1996 November z-band and the 1998 March r-band images. In the case of this star (all three components of which are included in Table 1), there was also a faint field star about 9″ to the northwest. This star's relative offset between these epochs changed approximately 1″, consistent with the 0.″459 yr^{-1} proper motion.

7.3. *LP 476-207*

LP 476-207, an M4 star, was given a photometric parallax of 142 mas in the CNS3. The subsequent *Hipparcos* measurement of 31.20 mas places it well outside the 8 pc sample. Part of the reason that the photometric parallax is so incorrect must be due to the presence of the companion we have found. Even though this star is no longer in the 8 pc

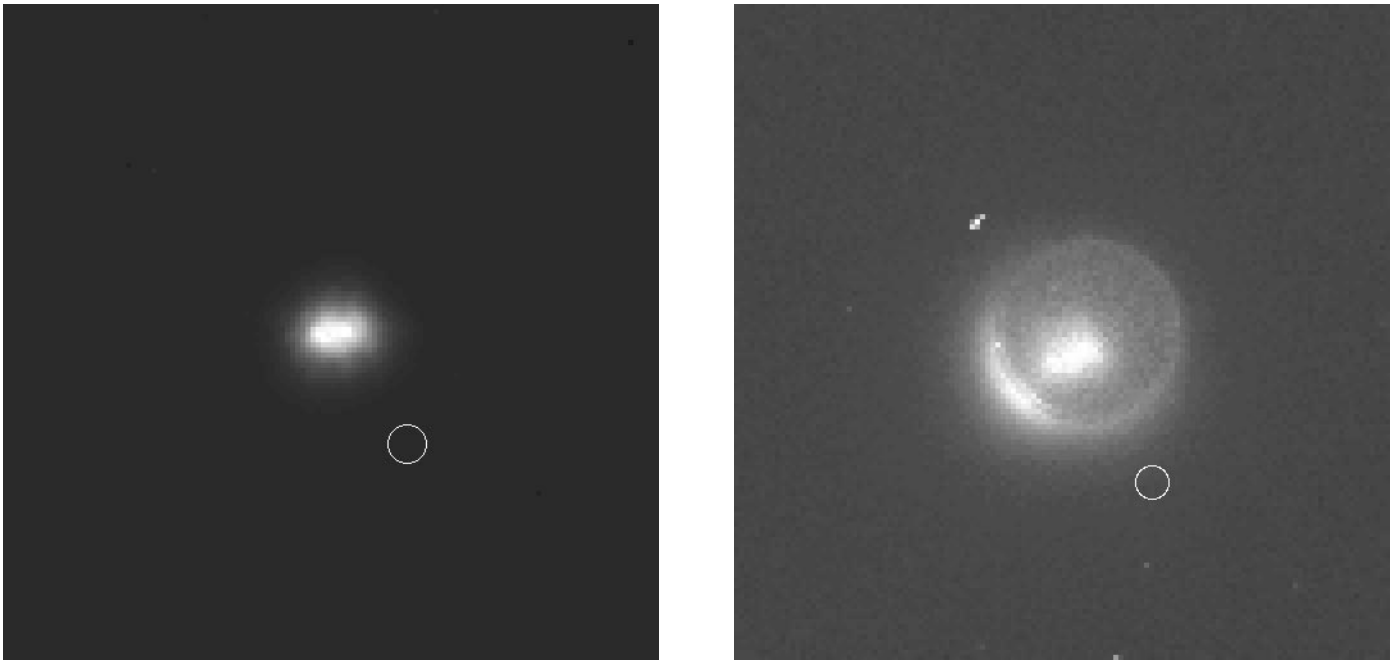

FIG. 10.—Images of G089-032 (162.00). This star has been resolved into two components. *Left*: A 5 s K-band image taken in 1996 December. The components have a separation of 0.″75, and north is up with east to the left. *Right*: A 1000 s z-band image taken in 1998 January. North is 4.°2 left of the top, and east is 90° counterclockwise from there. The two components have been resolved through the semitransparent coronagraphic mask (4.″3 in diameter). Here the components have a measured separation of 0.″71, consistent, within the 0.″05 error bars, with the infrared offset measured 1.1 yr earlier. The star has a known proper motion of 0.″354 yr^{-1}. Thus this is a common proper motion pair. The circle in each panel indicates the size of the core of a single star's point-spread function.

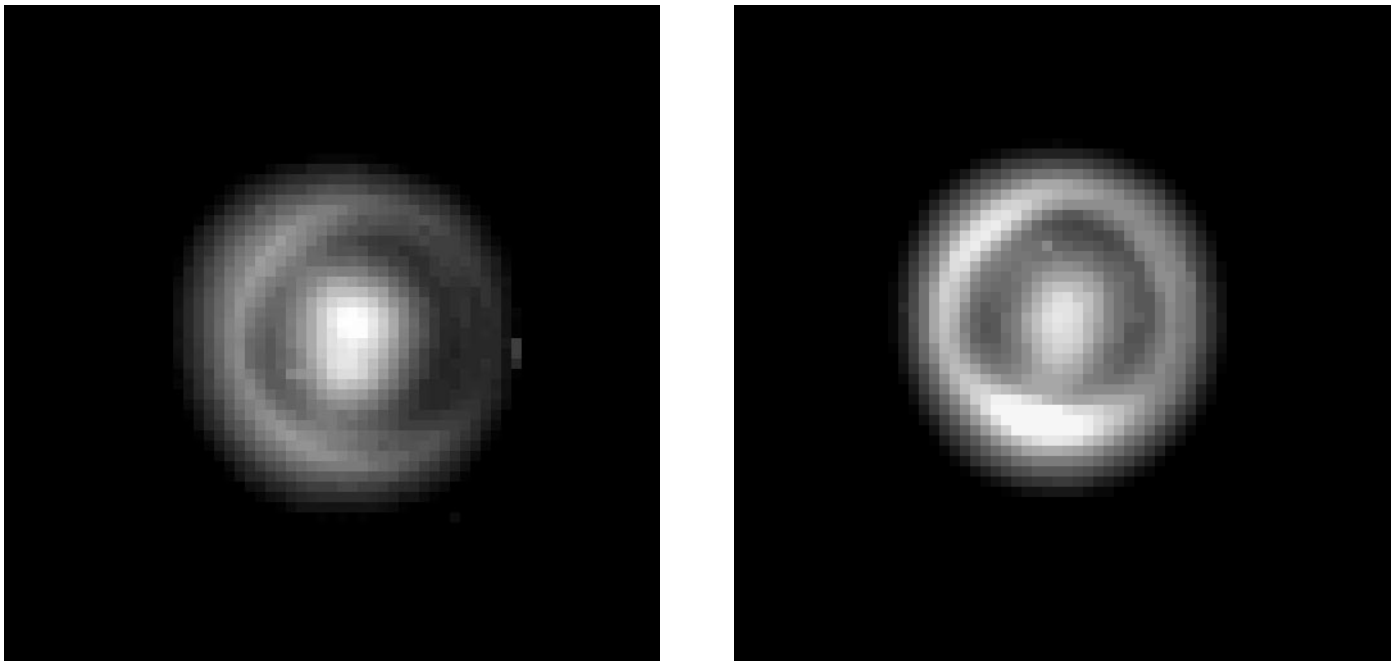

FIG. 11.—Images of G041-014. This star has been resolved into two components. *Left*: A 1000 s *z*-band image taken in 1996 November. The components have a separation of 0.″47 ± 0.″05. North is to the left and east is up. *Right*: A 1000 s *r*-band image taken in 1998 March. North is to the left and east is up. The two components have been only marginally resolved here through the semitransparent coronagraphic mask (4.″3 in diameter), the edge of which is visible because of the spillover of light from the stars. Here the components have a measured separation of 0.″52 ± 0.″1, consistent, within the error bars, with the offset measured 1.25 yr earlier. The star has a known proper motion of 0.″459 yr^{-1}. Thus, this is a common proper motion pair.

sample, it was in our original catalog, so we observed it. We found a common proper motion companion about 1 mag fainter in the *K* band than the primary star. This companion is located 1.″03 from LP 476-207. The two images in Figure 12 show a 5 s *K*-band image from 1996 October and a 1000 s *z*-band image from 1998 January. The proper motion of this star is only 0.″0837 yr^{-1}, which is less than 1 pixel yr^{-1} in these images, but the 2.24 yr baseline permits

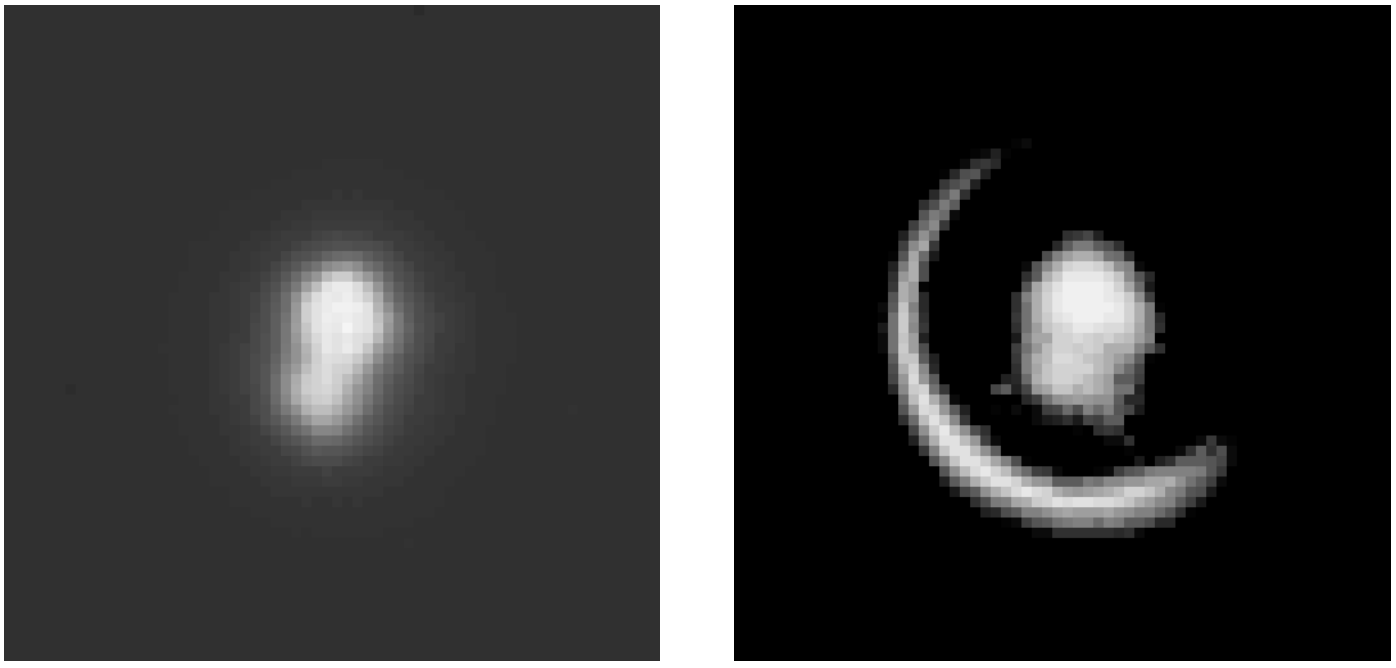

FIG. 12.—Images of LP 476-207. This star has been resolved into two components. *Left*: A 5 s *K*-band image taken in 1996 October. The components have a separation of 1.″03. North is up and east is to the left. *Right*: A 1000 s *z*-band image taken in 1998 January. North is up and east is to the left. The two components have been resolved through the semitransparent coronagraphic mask (4.″3 in diameter), the edge of which is visible because of the spillover of light from the companion. Here the components have a measured separation of 0.″99, consistent, within the 0.″05 error bars, with the infrared offset measured 2.24 yr earlier. The star has a known proper motion of 0.″0837 yr^{-1}. Thus, this is a common proper motion pair.

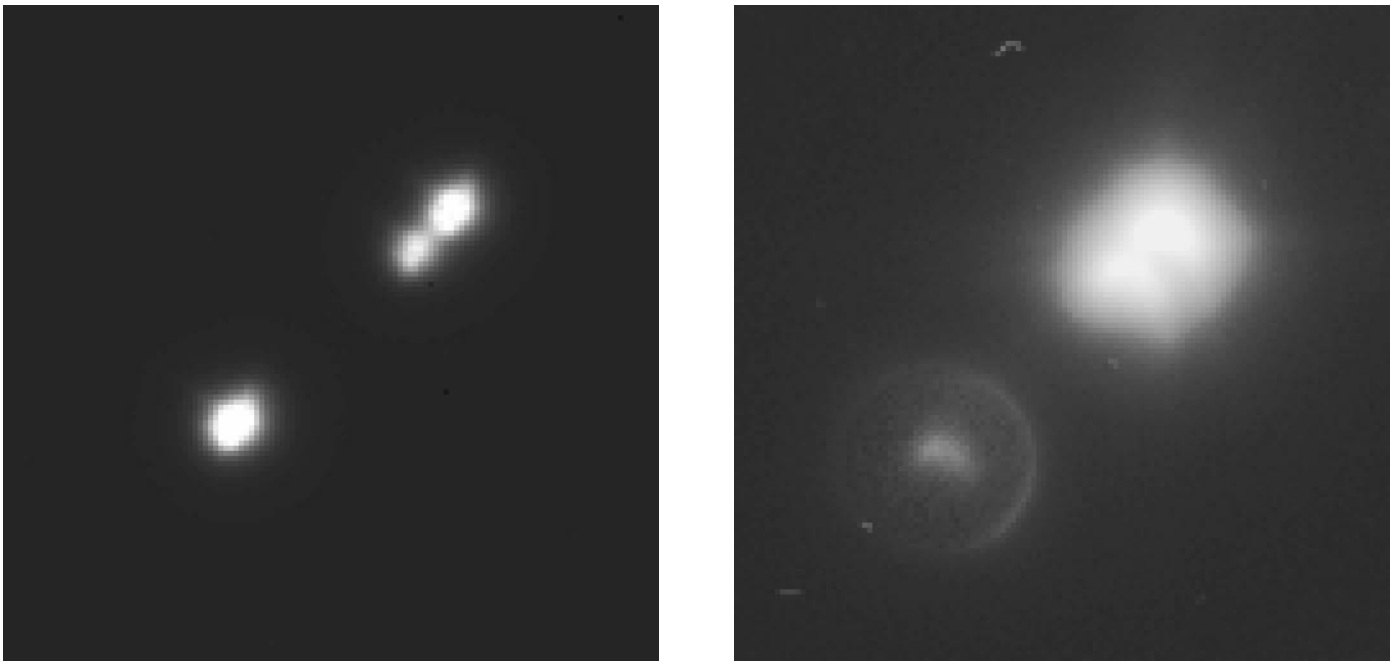

FIG. 13.—Images of the LP 771-095 triple system. This star is a known binary (the two outer stars), but we have found a third stellar component of the system that shares the proper motion of the other two (LP 771-095 and LP 771-096). *Left*: A 5 s *K*-band image taken in 1996 October. The components have a separation of 1.″12 and 7.″23 from the star LP 771-095, which is to the upper right in the images. North is up and east is to the left. *Right*: A 1000 s *z*-band image taken in 1995 October. North is up and east is to the left. LP 771-096 is under the mask in this case. All three components are clearly visible. Unfortunately, the astigmatism of the Palomar 60 inch telescope is also apparent. In order to measure accurate astrometry on this image, we used only the light in the brightest part of the point-spread function. Our astrometry matches that from the infrared images. The proper motion of the outer pair of stars has been measured to be 0.″4723 yr^{-1}. Thus, this is a common proper motion triple system.

easy identification of this fainter object as a common proper motion companion. Henry et al. (1997) also identified this star as double, without further information to determine that the two are physically associated. Delfosse et al. (1999) have confirmed the results above, measuring an offset of 0.″97 and a magnitude difference of 0.9 in the *K* band. However, because of the single-epoch nature of their observation, they were unable to state with certainty that this was

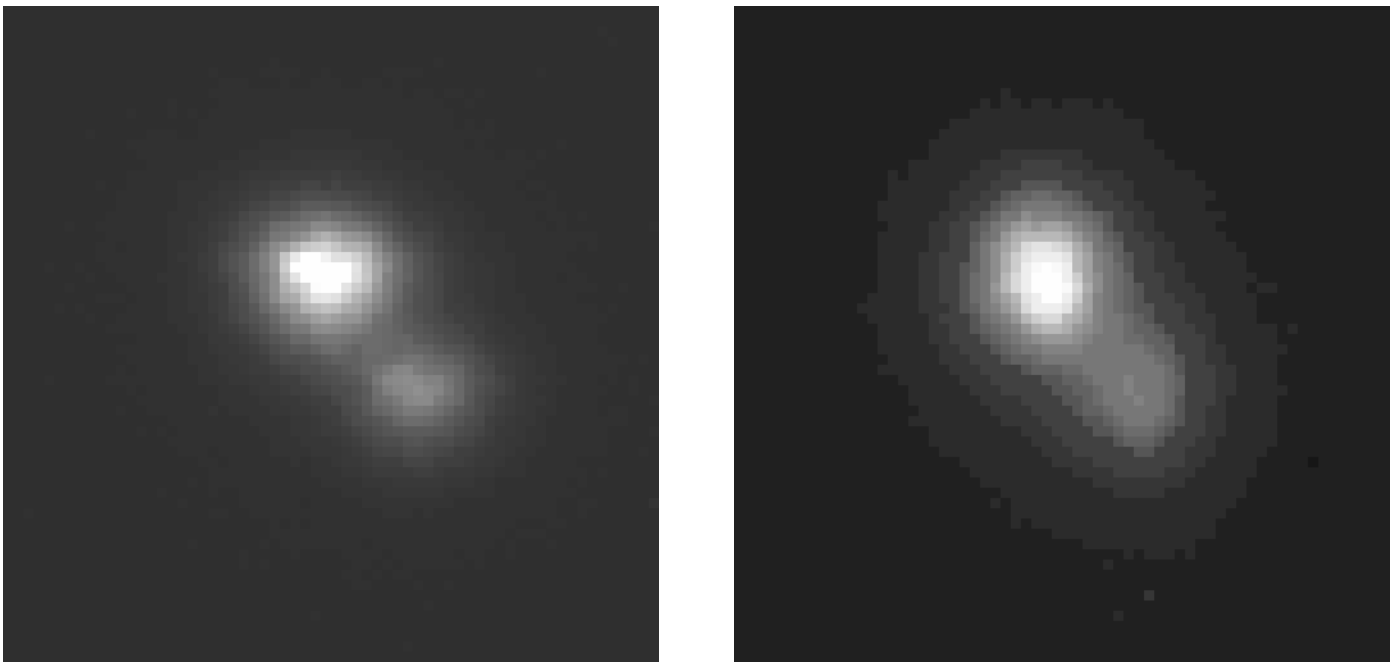

FIG. 14.—Images of LHS 1885. The second, fainter point source in these images is a common proper motion companion of LHS 1885, the brighter star. *Left*: A 5 s *K*-band image taken in 1995 November. The components have a separation of 1.″65, and north is up with east to the left. *Right*: A 5 s *K*-band image taken in 1996 December. North is up and east is to the left. The separation measured from this image is 1.″68. The proper motion of LHS 1885 is 0.″516 yr^{-1}. Therefore, the fainter star is a common proper motion companion of LHS 1885.

a physical companion of the star. Interestingly, they also reported the detection of an unresolved spectroscopic companion of the primary star.

7.4. *LP 771-095* (*LTT 1445*)

LP 771-095, along with LP 771-096, is a known binary, but we have found a third component that sits along the line between the two stars and shares the proper motion of the binary. The CNS3 listed a photometric parallax of 131 mas, but the *Hipparcos* mission subsequently measured the trigonometric parallax at 92.97 mas. The proper motion of this star is $0\farcs4723\ \mathrm{yr}^{-1}$, which makes identification of common proper motion companions easy within a single year. The stars LP 771-095 and LP 771-096 were both classified as M3.5 by Reid, Hawley, & Gizis (1995), and the third component is approximately 1.2 mag fainter than LP 771-095 in the K band. It has a separation of $1\farcs12$ from LP 771-095. LP 771-096 is $7\farcs23$ from LP 771-095. Figure 13 shows two of the images we acquired of this system.

7.5. *LHS 1885* (*G250-031*)

The CNS3 listed LHS 1885 with a photometric parallax of 129 mas. The Yale trigonometric parallax survey, however, measured a parallax of 87.4 mas, which removed it from our original sample of 8 pc stars. This M4.5 (Reid et al. 1995) star was reported as double by Henry et al. (1997). We have found that the second component shares the proper motion of the star. The second component is approximately 1.7 mag fainter in the K band and is $1\farcs66$ distant from the primary star. The proper motion of $0\farcs516\ \mathrm{yr}^{-1}$ permits identification of the common proper motion companion in less than a year. Figure 14 shows two K-band images taken in 1995 November and 1996 December.

8. SENSITIVITY TO BROWN DWARF COMPANIONS

We now must expand the analysis from § 6 to fainter levels and different colors: those of the brown dwarfs. The use of Gl 229B photometry (Matthews et al. 1996) permits the production of a table similar to Table 9, but for cool brown dwarf companions. This is presented in Table 10. We use Gl 229B as a template cool brown dwarf because, of all the cool brown dwarfs, it is the most comprehensively studied (Oppenheimer et al. 1998). The only other one with a known parallax is Gliese 570D (Burgasser et al. 2000), but its photometry is not as comprehensively measured.

The contrast between Tables 10 and 9 is quite dramatic. The survey has no sensitivity to cool brown dwarfs in the r band. This is principally because in this band the absolute magnitude of the template brown dwarf, Gl 229B, is 24.6 (Golimowski et al. 1998), while the images were limited to, at best, 21.7. The survey is most sensitive to brown dwarf companions in the z band at the wider separations and in the J band for separations ≤ 40 AU. This is due to the suppression of the broad wings of the point-spread function by the pupil-plane coronagraphic stop. Brown dwarfs in orbits with separations between 50 and 100 AU would have been detected around more than 80% of the stars in the survey.

Ultimately we would like to express the sensitivity of the survey in terms of what the lowest mass brown dwarf we could possibly detect is. This is complicated by the fact that brown dwarfs cool. As such, a brown dwarf of a given mass will evolve through many magnitudes of brightness in a given bandpass over a timescale of several gigayears. Unfortunately, the state-of-the-art models that produce synthetic spectra, and thus color information, do not extend to the r band. However, the models of Burrows et al. (1997; Burrows, Marley, & Sharp 2000; A. Burrows 1999, private communication) supply us with the magnitudes in the z and J bands for brown dwarfs of all masses ($15M_J$ to $70M_J$) for two different ages, 1 and 5 Gyr. From this information, we can convert the absolute magnitudes in Tables 7 and 6 into brown dwarf masses for each of the two ages, 1 and 5 Gyr. The results are shown in tabular and graphical form: Tables 11 through 14 and Figures 15 through 18.

We should note that the two ages chosen here are unfortunately not perfectly representative of the ages of the sample stars. Assuming a constant star formation rate in the galaxy, the ages of stars in the disk would be evenly distributed between 0 and 10 Gyr. Unfortunately, we do not have model flux densities for 10 Gyr objects.

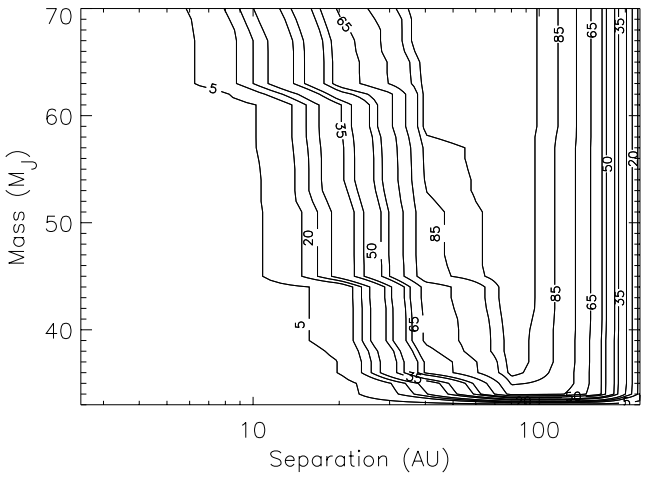

FIG. 15.—Brown dwarf mass vs. separation: survey coverage in z, age 5 Gyr. This is a contour plot of an expanded form of the data presented in Table 11. It shows the survey sensitivity in the z band as described in the text as a function of brown dwarf mass and orbital separation, assuming the age of the stars is 5 Gyr.

TABLE 10

PERCENTAGE OF SURVEY STARS WITH OBSERVATIONS IN J, z, AND r SENSITIVE TO GLIESE 229B–LIKE COMPANIONS

	SEPARATION (AU)									
BAND	2.5	5	10	20	40	80	120	160	200	225
J.....	0	5	37	70	77	50	2	0	0	0
z.....	0	0	0	5	55	92	82	59	26	13
r.....	0	0	0	0	0	0	0	0	0	0

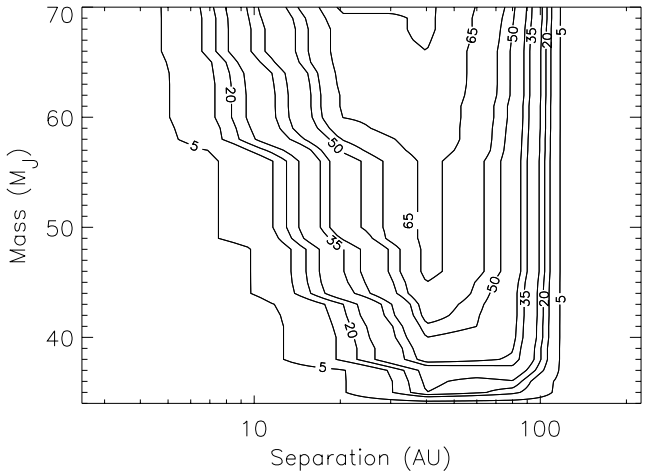

FIG. 16.—Same as Fig. 15, but in *J*. This is a contour plot of an expanded form of the data presented in Table 12.

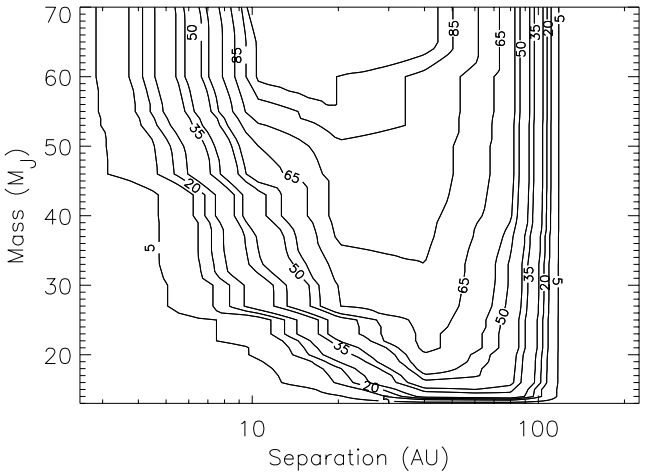

FIG. 18.—Same as Fig. 17, but in *J*. This is a contour plot of an expanded form of the data presented in Table 14.

Caveat.—We do not separately evaluate the conversion between *J* magnitudes and mass and *K*-band magnitudes and mass, because the measurements in the two bands yield essentially identical masses. As we mentioned above (§ 6), the sensitivity curves for the *K* band are the same as those for *J*.

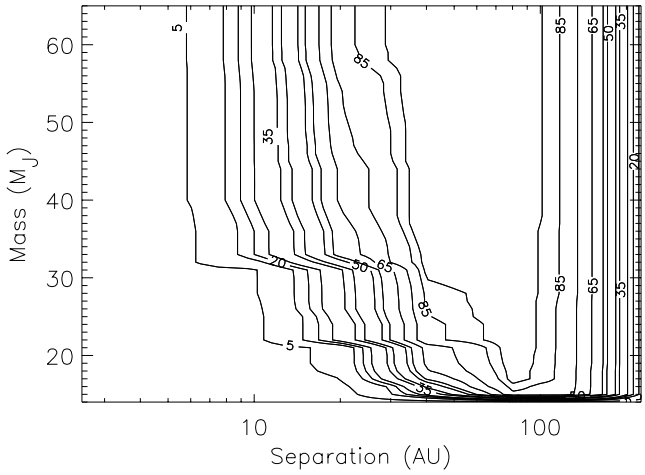

FIG. 17.—Brown dwarf mass vs. separation: survey coverage in *z*, age 1 Gyr. This is a contour plot of an expanded form of the data presented in Table 13. It shows the survey sensitivity in the *z* band as described in the text as a function of brown dwarf mass and orbital separation, assuming the age of the stars is 1 Gyr.

9. DISCUSSION AND SUMMARY

What is becoming increasingly clear from the searches for field brown dwarfs, such as the Two Micron All-Sky Survey (2MASS; Reid et al. 1999), is that brown dwarfs greatly outnumber stars in the field population. It would seem to follow logically that many stars could have brown dwarf companions, if the formation mechanism for binary stars applies to star–brown dwarf systems. However, we have shown here that brown dwarfs seem to have a multiplicity fraction with stars far below the 17% to 30% observed for all stars (Reid & Gizis 1997). Between 40 and 100 AU, we would have detected brown dwarfs more massive than $40M_J$ around 80% of the survey stars. The only other cool brown dwarf companion of a star within 8 pc is Gl 570D (Burgasser et al. 2000). We did not detect this object because the separation is $\sim 4'$, placing it outside our field of view.

The initial goal of this survey was to find brown dwarfs. However, because we found only one, and because our survey detection limits are complex functions of brightness, separation, and age, placing constraints on possible mass and separation distributions of brown dwarf companions requires extensive Monte Carlo simulations. This is a rather

TABLE 11

PERCENTAGE OF SURVEY STARS WITH *z*-BAND OBSERVATIONS SENSITIVE TO COMPANIONS OF BROWN DWARF MASS: AGE = 5 Gyr

MASS (M_J)	SEPARATION (AU)									
	2.5	5	10	20	40	80	120	160	200	225
70.....	0	1	25	67	98	95	84	60	26	13
65.....	0	0	20	59	93	95	84	60	26	13
59.....	0	0	4	34	92	95	84	60	26	13
51.....	0	0	3	28	83	95	83	60	26	13
45.....	0	0	3	28	82	95	83	60	26	13
39.....	0	0	1	8	67	93	83	59	26	13
35.....	0	0	0	1	28	86	82	59	26	13
34.....	0	0	0	1	24	79	76	59	25	13
33.....	0	0	0	0	0	0	0	0	0	0

NOTE.—Here M_J is the mass of Jupiter.

TABLE 12

PERCENTAGE OF SURVEY STARS WITH J-BAND OBSERVATIONS SENSITIVE TO COMPANIONS OF BROWN DWARF MASS: AGE = 5 Gyr

MASS (M_J)	SEPARATION (AU)									
	2.5	5	10	20	40	80	120	160	200	225
70.....	0	5	39	77	77	52	2	0	0	0
60.....	0	4	28	65	73	48	2	0	0	0
50.....	0	1	9	46	68	46	2	0	0	0
45.....	0	1	5	33	65	44	2	0	0	0
40.....	0	1	1	16	50	42	2	0	0	0
35.....	0	0	0	4	25	17	1	0	0	0
34.....	0	0	0	0	0	0	0	0	0	0

NOTE.—Here M_J is the mass of Jupiter.

complex problem that requires its own computational techniques. This work is currently in progress and will be published in a separate paper.

Here we present several simple statements that can be made with certainty:

1. This survey would have found all stellar companions of any type around 98% of the survey stars and between 3″ and 30″ of the stars. Indeed, in § 7 we present six new stellar companions. This does not dramatically change the multiplicity fraction for the 8 pc sample.

2. Brown dwarfs more massive than $40M_J$, at least as old as 5 Gyr, would have been detected around 80% of the survey stars for separations between 40 and 120 AU. Only one such object exists (Gl 229B, at over 39 AU), implying a binary fraction of around 1%, assuming that Gl 229B is a prototypical brown dwarf. (We must note here that the exclusion of models of older brown dwarfs in this assertion must be considered when interpreting the result. A proper assessment of the constraints provided by our survey on the binary fraction of brown dwarfs really requires extensive modeling of the possible populations of stars and brown dwarf companions.)

3. There has been no complete assessment of the population of brown dwarf companions of the survey stars for separations outside 100 AU. The most complete study to date has been that of Simons et al. (1996), but it did not cover the whole sample and turned up no new brown

TABLE 13

PERCENTAGE OF SURVEY STARS WITH z-BAND OBSERVATIONS SENSITIVE TO COMPANIONS OF BROWN DWARF MASS: AGE = 1 Gyr

MASS (M_J)	SEPARATION (AU)									
	2.5	5	10	20	40	80	120	160	200	225
65.....	0	1	26	83	99	97	84	60	26	13
60.....	0	1	26	83	99	97	84	60	26	13
51.....	0	1	25	74	98	97	84	60	26	13
40.....	0	1	25	67	98	97	84	60	26	13
31.....	0	0	4	34	92	95	84	60	26	13
21.....	0	0	1	8	69	95	83	60	26	13
15.....	0	0	0	1	28	83	81	59	26	13
14.....	0	0	0	0	0	0	0	0	0	0

NOTE.—Here M_J is the mass of Jupiter.

TABLE 14

PERCENTAGE OF SURVEY STARS WITH J-BAND OBSERVATIONS SENSITIVE TO COMPANIONS OF BROWN DWARF MASS: AGE = 1 Gyr

MASS (M_J)	SEPARATION (AU)									
	2.5	5	10	20	40	80	120	160	200	225
70.....	1	30	96	94	94	59	2	0	0	0
60.....	1	30	91	90	83	59	2	0	0	0
50.....	1	18	64	83	81	58	2	0	0	0
40.....	0	5	46	80	78	56	2	0	0	0
30.....	0	4	28	66	74	49	2	0	0	0
25.....	0	1	9	46	71	46	2	0	0	0
20.....	0	1	5	31	64	44	2	0	0	0
16.....	0	1	1	16	48	42	2	0	0	0
13.....	0	0	0	0	0	0	0	0	0	0

NOTE.—Here M_J is the mass of Jupiter.

dwarfs. Our survey is insensitive to such wide-separation binaries. However, the 2MASS project (Burgasser et al. 2000) should reveal all companions of the known nearby stars with wide separations that are similar to or hotter than Gl 229B.

4. A more sensitive survey of the same stars in the sample presented here is necessary to obtain a complete census of brown dwarf companions in the solar neighborhood. This requires the suppression of scattered light from the primary stars (i.e., achieving a higher dynamic range) and an increase in the limiting magnitude of the sky-limited regions of the images. The next step in this sort of research is a full-scale, adaptive optics–based survey, ideally with simultaneous infrared and optical imaging.

9.1. *Endnote*

In § 4, we addressed the issue of how sensitive the survey is as a whole and for individual stars. Ideally, these calculations and observations should be gathered into a general statement about brown dwarf companions of nearby stars. This turns out to be a rather complex problem with a large and essentially unexplored parameter space. Not only is it unexplored from the observational standpoint, but essentially no research has been conducted on the theoretical aspects of the problem.

From the observational standpoint, the search for faint or low-mass companions of stars has become practical only in the past 5 to 10 years. The two approaches to the problem—direct and indirect detection—have turned up positive results, but each has access to a different part of the parameter space. The parameter space is defined by the mass of the companion and orbital separation. This seems simple enough, but as shown in the previous section, the sensitivity of a direct observing campaign is not a constant through any region of this parameter space when the mass is below the "hydrogen-burning limit." This is particularly true because brown dwarfs cool. The cooling essentially introduces an additional parameter, the age. In the case of the indirect searches, the sensitivity to mass is uninfluenced by age, but the parameter space is also explored in a nonuniform manner for a large sample of stars: it depends mainly upon the length of time over which the observations are scattered for each star and how they are distributed in time. For example, periodic observations will be completely insensitive to objects that orbit with a multiple of the period of observation. The point of this discussion is that the mass-separation parameter space is poorly sampled, and making direct comparisons between the direct and indirect observing methods is difficult because the overlap in parameter space is only now beginning to exist. The simplest comparison is shown in Figure 19, where the mass-separation parameter space is shown with lines indicating sensitivity limits of various search techniques. The only complete imaging survey on the plot is that presented in this paper.

The only certain statement we can make at this time is that the multiplicity fraction of brown dwarfs is far smaller than the 35% to 40% for stellar binary systems. In light of this, it is important to discuss the mass function. The mass function below the "hydrogen-burning limit" has been the subject of heated debate and has mainly relied upon observational rather than theoretical constraints (i.e., this part of the mass function cannot be calculated theoretically at present). In the past 10 years it has become clear that the Salpeter mass function, which works for higher mass stars, does not apply to the very lowest mass stars. Recently, studies of open star clusters such as the Pleiades, which probe into the brown dwarf mass range, have begun to provide extensions of the mass function (see, e.g., Martín, Zapatero Osorio, & Rebolo 1998). However, the masses of the objects discovered are generally not well constrained, because the theoretical models of these objects are not complete and are unable to reproduce all of the observations. Other techniques for finding brown dwarfs in the field, such as the microlensing experiments, give accurate masses but have found such a sparse number of objects in the brown dwarf mass range that the error bars on the implied mass distribution are large. A careful analysis of the MACHO results (Alcock et al. 1998) is presented by Chabrier & Méra (1998) and "clearly illustrates the difficulty to reach robust conclusions about the mass in the form of substellar objects in the central regions of the Galaxy, and more precisely, in the disk and the bulge, from present microlensing experiments." Indeed, Chabrier & Méra cannot constrain the space density of brown dwarfs to a range smaller than an order of magnitude around $9 \times 10^{-3}\, M_{\odot}\, \mathrm{pc}^{-3}$.

A further complication of this problem stems from the observation, most recently by Reid & Gizis (1997) and Reid et al. (1999), that the mass function for companions is actually different from the mass function of field stars. In their analysis of the 8 pc sample, they find that the distribution of the mass ratios of multiple systems has a significant peak near 0.95. In their estimation, this excludes the notion

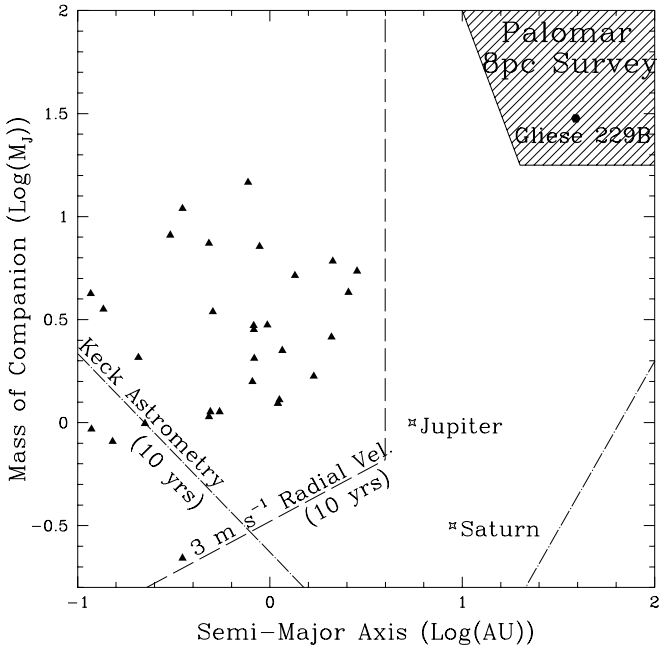

FIG. 19.—Mass-separation parameter space. This plot shows the known substellar companions of stars discovered to date. Jupiter and Saturn are indicated and labeled. Gl 229B is represented by a circle. The planets found in radial velocity searches are represented by triangles. The curves indicate the detection limits of several techniques. The dashed line shows the 3 m s^{-1} limit of the current radial velocity searches with baselines of 10 yr. The dash-dotted lines show the predicted limits of an astrometric search using the Keck interferometer project over a 10 yr period of observations. Our survey probed the hatched region in the upper right. Our work represents the first direct-imaging project to probe this parameter space.

that companions of stars come from the same mass function as solitary stars. For a survey of the nature presented here, this makes drawing conclusions about the various mass functions described above essentially irrelevant. It would be akin to trying to understand "techno" music by listening to classical violin concerti. There has been no study of companion mass functions in the brown dwarf regime. Furthermore, if the mass ratio distribution that Reid & Gizis (1997) find extends into the brown dwarf mass range, our survey excludes the most important set of stars for which to find brown dwarf companions: We argued that the 25% incompleteness of our sample is all due to missing the very lowest mass stars within 8 pc. These are the ones that would be expected to have more brown dwarf companions.

REFERENCES

Alcock, C., et al. 1998, ApJ, 499, L9
Burgasser, A. J. et al. 2000, ApJ, 531, L57
Burrows, A., & Liebert, J. 1993, Rev. Mod. Phys., 65, 301
Burrows, A., et al. 1997, ApJ, 491, 856
Burrows, A., Marley, M. S., & Sharp, C. M. 2000, ApJ, 531, 438
Chabrier, G., & Méra, D. 1998, in ASP Conf. Ser. 134, Brown Dwarfs and Extrasolar Planets, ed. R. Rebolo, E. L. Martín, & M. R. Zapatero Osorio (San Francisco: ASP), 495
Cudworth, K. M. 1976, AJ, 81, 519
———. 1979, AJ, 84, 1866
Delfosse, X., Forveille, T., Beuzit, J.-L., Udry, S., Mayor, M., & Perrier, C. 1999, A&A, 344, 897
Delfosse, X., Forveille, T., Mayor, M., Perrier, C., Naef, D., & Queloz, D. 1998, A&A, 338, L67
Gizis, J. E., Monet, D. G., Reid, I. N., Kirkpatrick, J. D., Liebert, J., & Williams, R. J. 2000, AJ, 120, 1085
Gliese, W., & Jahreiss, H. 1991, Preliminary Version of the Third Catalogue of Nearby Stars (NSSDC/ADC Cat. 5070A) (Greenbelt, MD: GSFC) (CNS3)
Golimowski, D. A., Burrows, C. J., Kulkarni, S. R., Oppenheimer, B. R., & Brukardt, R. A. 1998, AJ, 115, 2579
Golimowski, D. A., Clampin, M., Durrance, S. T., & Barkhouser, R. H. 1992, Appl. Opt., 31, 4405
Golimowski, D. A., Nakajima, T., Kulkarni, S. R., & Oppenheimer, B. R. 1995, ApJ, 444, L101
Henry, T. J., Ianna, P. A., Kirkpatrick, J. D., & Jahreiss, H. 1997, AJ, 114, 388
Henry, T. J., & McCarthy, D. W., Jr. 1990, ApJ, 350, 334
———. 1993, AJ, 106, 773
Koerner, D. W., Kirkpatrick, J. D., McElwain, M. W., & Bonaventure, N. R. 1999, ApJ, 526, L25
Luyten, W. J. 1977, Proper Motion Survey with the 48-Inch Schmidt Telescope, Vol. 50 (Minneapolis: Univ. Minnesota)
Lyot, M. B. 1939, MNRAS, 99, 580
Martín, E. L., Zapatero Osorio, M. R., & Rebolo, R. 1998, in ASP Conf. Ser. 134, Brown Dwarfs and Extrasolar Planets, ed. R. Rebolo, E. L. Martín, & M. R. Zapatero Osorio (San Francisco: ASP), 507
Matthews, K., Nakajima, T., Kulkarni, S. R., & Oppenheimer, B. R. 1996, AJ, 112, 1678
McCaughrean, M. J., & Stauffer, J. R. 1994, AJ, 108, 1382
Nakajima, T., Durrance, S. T., Golimowski, D. A., & Kulkarni, S. R. 1994, ApJ, 428, 797
Nakajima, T., Oppenheimer, B. R., Kulkarni, S. R., Golimowski, D. A., Matthews, K., & Durrance, S. T. 1995, Nature, 378, 463
Oppenheimer, B. R., Kulkarni, S. R., Matthews, K., & Nakajima, T. 1995, Science, 270, 1478
Oppenheimer, B. R., Kulkarni, S. R., Matthews, K., & van Kerkwijk, M. H. 1998, ApJ, 502, 932
Oppenheimer, B. R., Kulkarni, S. R., & Stauffer, J. R. 2000, in Protostars and Planets IV, ed. V. Mannings, A. P. Boss, & S. S. Russell (Tucson: Univ. Arizona Press), 1313
Perryman, M. A. C., et al. 1997, A&A, 323, L49
Reid, I. N., & Gizis, J. E. 1997, AJ, 113, 2246
Reid, I. N., Hawley, S. L., & Gizis, J. E. 1995, AJ, 110, 1838
Reid, I. N., et al. 1999, ApJ, 521, 613
Schroeder, D. J., et al. 2000, AJ, 119, 906
Simons, D. A., Henry, T. J., & Kirkpatrick, J. D. 1996, AJ, 112, 2238
Skrutskie, M. F., Forrest, W. J., & Shure, M. 1989, AJ, 98, 1409
van Altena, W. F., Lee, J. T., & Hoffleit, E. D. 1995, The General Catalogue of Trigonometric Stellar Parallaxes (4th ed.; New Haven: Yale Univ. Obs.)
Van Biesbroeck, G. 1961, AJ, 66, 528
Weis, E. W. 1984, ApJS, 55, 289